

South Dakota State University

## Open PRAIRIE: Open Public Research Access Institutional Repository and Information Exchange

---

Electronic Theses and Dissertations

---

1978

### Rotaviral Enteritis in Gnotobiotic Pigs: A Scanning Electron Microscopic Study

Marcus W. Johnshoy

Follow this and additional works at: <https://openprairie.sdstate.edu/etd>



Part of the [Microbiology Commons](#)

---

#### Recommended Citation

Johnshoy, Marcus W., "Rotaviral Enteritis in Gnotobiotic Pigs: A Scanning Electron Microscopic Study" (1978). *Electronic Theses and Dissertations*. 5570.  
<https://openprairie.sdstate.edu/etd/5570>

This Thesis - Open Access is brought to you for free and open access by Open PRAIRIE: Open Public Research Access Institutional Repository and Information Exchange. It has been accepted for inclusion in Electronic Theses and Dissertations by an authorized administrator of Open PRAIRIE: Open Public Research Access Institutional Repository and Information Exchange. For more information, please contact [michael.biondo@sdstate.edu](mailto:michael.biondo@sdstate.edu).

ROTAVIRAL ENTERITIS IN GNOTOBIOTIC PIGS:

A SCANNING ELECTRON MICROSCOPIC STUDY

BY

MARCUS W. JOHNSHOY

A thesis submitted  
in partial fulfillment of the requirements for the  
degree Master of Science, Department of  
Microbiology, South Dakota State  
University

1978

SOUTH DAKOTA STATE UNIVERSITY LIBRARY

ROTAVIRAL ENTERITIS IN GNOTOBIOTIC PIGS:

A SCANNING ELECTRON MICROSCOPIC STUDY

This thesis is approved as a creditable and independent investigation by a candidate for the degree, Master of Science, and is acceptable as meeting the thesis requirements for this degree, but without implying that the conclusions reached by the candidate are necessarily the conclusions of the major department.

John McAdaragh, Thesis Advisor

Date

T. Ross Wilkinson  
Head, Microbiology Department

Date

#### ACKNOWLEDGEMENTS

I would like to extend my appreciation to Dr. Mahlon Vorhies for providing facilities for parts of this study and to the Cooperative State Research Service, Department of Agriculture, for providing funding for this project. I am grateful to Mr. John McAdaragh, my thesis advisor, and to Dr. Martin Bergland for help and suggestions during the course of this study and during preparation of this manuscript. Thanks are also due to Dr. Clyde Kirkbride for assistance in reviewing this manuscript. I would also like to thank Dr. R. C. Myer, College of Veterinary Medicine, University of Illinois for providing the gnotobiotic piglets, and Melva Managan for preparation of tissues for light microscopy. I would like to thank the Microbiology Department for the cooperation extended to the Veterinary Science Department in my graduate studies. Finally, special thanks to Dr. Robert Hammer, College of Veterinary Medicine, University of Minnesota, for his instruction and guidance on the use of the scanning electron microscope, without which this project would not have been possible.

MWJ



## TABLE OF CONTENTS

	Page
INTRODUCTION . . . . .	1
LITERATURE REVIEW . . . . .	3
Normal Anatomy of the Small Intestine . . . . .	3
Intestinal Layers . . . . .	3
Villi . . . . .	4
Epithelium . . . . .	4
Microvilli . . . . .	6
Rotaviruses . . . . .	6
Scanning Electron Microscopy . . . . .	9
Introduction . . . . .	9
Principles of Scanning Electron Microscopy . . . . .	9
Specimen Preparation . . . . .	10
Fixation and Dehydration . . . . .	10
Drying . . . . .	11
Application of Metal Surface . . . . .	12
Scanning Electron Microscopic Description of the Small Intestine . . . . .	12
Villi . . . . .	12
Epithelium . . . . .	13
Microvilli . . . . .	14
Observations on Rotaviral Infections . . . . .	14
MATERIALS AND METHODS . . . . .	16
Gnotobiotic Pigs . . . . .	16
Inoculum . . . . .	16
Inoculation and Specimen Collection . . . . .	16
Light Microscopic Examination . . . . .	17
Scanning Electron Microscopic Examination . . . . .	17
RESULTS . . . . .	22
Trial 1 . . . . .	22
12 Hours . . . . .	22
24 Hours . . . . .	33
36 Hours . . . . .	42
48 Hours . . . . .	49
60 Hours . . . . .	49
72 Hours . . . . .	54
84 Hours . . . . .	65
96 Hours . . . . .	74
Trial 2 . . . . .	85
DISCUSSION . . . . .	86
SUMMARY . . . . .	99
LITERATURE CITED . . . . .	101

# LIST OF FIGURES

Figure	Page
1. Scanning electron micrograph of the lower jejunum 12 hours post inoculation (PI) . . . . .	26
2. Scanning electron micrograph of the control lower jejunum at 24 hours . . . . .	26
3. Light micrograph of the lower jejunum 12 hours PI . . . . .	28
4. Light micrograph of the control lower jejunum at 24 hours . . . . .	28
5. Scanning electron micrograph of the lower ileum 12 hours PI . . . . .	30
6. Scanning electron micrograph of a single lower ileum villus from the 24 hour control pig . . . . .	30
7. Light micrograph of the lower ileum 12 hours PI . . . . .	32
8. Light micrograph of the control lower ileum at 24 hours . . . . .	32
9. Scanning electron micrograph of the lower jejunum 24 hours PI . . . . .	35
10. Light micrograph of a single villus in the lower jejunum 24 hours PI . . . . .	35
11. Scanning electron micrograph of the duodenum 24 hours PI . . . . .	37
12. Scanning electron micrograph of the mid intestine 24 hours PI . . . . .	37
13. Scanning electron micrograph of the lower ileum 24 hours PI . . . . .	39
14. Scanning electron micrograph of the control lower ileum at 24 hours . . . . .	39
15. Light micrograph of the lower ileum 24 hours PI . . . . .	41
16. Scanning electron micrograph of the duodenum 36 hours PI . . . . .	44
17. Scanning electron micrograph of the control duodenum at 24 hours . . . . .	44
18. Light micrograph of the duodenum 36 hours PI . . . . .	46

# LIST OF FIGURES (continued)

Figure	Page
19. Light micrograph of the control duodenum at 24 hours . . .	46
20. Scanning electron micrograph of the lower ileum 36 hours PI . . . . .	48
21. Light micrograph of the lower ileum 36 hours PI . . . . .	48
22. Scanning electron micrograph of the mid intestine 48 hours PI . . . . .	51
23. Light micrograph of a mid intestinal villi 48 hours PI . .	51
24. Scanning electron micrograph of the upper ileum 48 hours PI . . . . .	53
25. Scanning electron micrograph of the mid intestine 60 hours PI . . . . .	53
26. Scanning electron micrograph of the upper jejunum 72 hours PI . . . . .	56
27. Scanning electron micrograph of normal jejunal villi 72 hours PI . . . . .	56
28. Light micrograph of the upper jejunum 72 hours PI . . . .	58
29. Light micrograph of the control upper jejunum at 72 hours .	58
30. Scanning electron micrograph of the mid intestine 72 hours PI . . . . .	60
31. Scanning electron micrograph of the upper ileum 72 hours PI . . . . .	60
32. Scanning electron micrograph from the upper ileum 72 hours PI of a rounded epithelial cell . . . . .	62
33. Scanning electron micrograph from the upper ileum 72 hours PI of a rounded epithelial cell . . . . .	62
34. Scanning electron micrograph of control microvilli . . . .	62
35. Scanning electron micrograph of the lower ileum 72 hours PI . . . . .	64

# LIST OF FIGURES (continued)

Figure	Page
36. Scanning electron micrograph of control lower ileum villi at 72 hours . . . . .	64
37. Scanning electron micrograph of the duodenum 84 hours PI . . . . .	67
38. Scanning electron micrograph of the lower jejunum 84 hours PI . . . . .	69
39. Light micrograph of the lower jejunum 84 hours PI . . . . .	69
40. Scanning electron micrograph of the mid intestine 84 hours PI . . . . .	71
41. Scanning electron micrograph of the upper ileum 84 hours PI . . . . .	71
42. Scanning electron micrograph of the upper ileum control at 96 hours . . . . .	73
43. Scanning electron micrograph of the upper jejunum 96 hours PI . . . . .	76
44. Light micrograph of the lower jejunum 96 hours PI . . . . .	76
45. Scanning electron micrograph of two rounded epithelial cells from the upper jejunum 96 hours PI . . . . .	78
46. Scanning electron micrograph of the mid intestine 96 hours PI . . . . .	80
47. Scanning electron micrograph of the mid intestine 96 hours PI . . . . .	80
48. Light micrograph of the mid intestine 96 hours PI . . . . .	82
49. Scanning electron micrograph of the control mid intestine at 96 hours . . . . .	82
50. Scanning electron micrograph of the lower ileum 96 hours PI . . . . .	84
51. Scanning electron micrograph of the control lower ileum at 96 hours . . . . .	84

## LIST OF TABLES

Table	Page
1. Number of the pigs and time after exposure the pig was euthanatized . . . . .	18
2. Scanning electron microscopic findings in the intestines of rotavirus infected gnotobiotic piglets . . . . .	23

## INTRODUCTION

Diarrhea has been an ever present problem for man and animals. An enormous amount of work has been done identifying various bacteria and viruses as causative agents and determining their pathogeneses. Transmissible gastroenteritis (TGE) virus and bovine viral diarrhea virus have been known for some time to cause diarrhea in pigs and cattle respectively. Reovirus-like agents, or rotaviruses, have recently been recognized as a cause of diarrhea. Epizootic diarrhea of mice was the first virus-induced diarrhea reported (17) whose etiologic agent was later classified as a rotavirus. In 1969, a similar virus was found to cause diarrhea in cattle (48). In 1976, rotaviruses were implicated in diarrhea of piglets (91,42). Complete characterization of the rotaviruses has been restricted because of their failure to adapt to cell lines commonly used for virus isolation and study.

Because the discovery of rotavirus infection in pigs is very recent, studies of the pathogenesis have been quite limited in both number and extent. The current research was designed to infect gnotobiotic pigs with rotavirus, and then to use scanning electron microscopy and light microscopy to determine the changes in the structure of the small intestine.

The objectives of this study were:

1. To experimentally reproduce rotaviral diarrhea in gnotobiotic pigs.
2. To determine the appearance of the normal intestine by scanning electron and light microscopy.

3. To compare by scanning electron and light microscopy the appearance of segments from different areas of intestine and to determine the development, location, and severity of rotaviral lesions in gnotobiotic pigs.

## LITERATURE REVIEW

### NORMAL ANATOMY OF THE SMALL INTESTINE

The principle functions of the small intestine are: 1, to move forward the chyme it receives from the stomach, 2, to continue digestion with juices secreted by its own glands and accessory glands, and 3, to absorb into the blood and lymph vessels in the mucosa the nutrient materials released by digestion (9).

#### Intestinal Layers

Sheehy and Floch (75) and Trautman and Fiebiger (86) have described the normal anatomy of the small intestine. The wall of the small intestine is divided into five layers: serous, muscle, submucosa, mucosal muscles, and mucosa. The tunica serosa comprises the outer coat of the small intestine and is derived from the peritoneum. The muscular coat, or tunica muscularis, consists of an outer longitudinal layer and an inner circular layer, and lies beneath the submucosal layer (75). The latter consists of loose fibrillar connective tissue, fat tissues, lymphoid tissues, autonomic ganglia, nerves, and vessels (86). Separating the submucosa from the mucosa is the muscularis mucosa, composed of circular and longitudinal smooth muscle fibers. The tunica mucosa is the luminal surface of the small intestine, consisting of the villi and the crypts of Lieberkuhn (75). The mucosal surface of the small intestine is characterized by large circular folds in the mucosa (the valves of Kerckring) and numerous finger-like projections called villi. Both serve to greatly increase the absorptive surface area (9).



### Villi

Pfeiffer (71) reported that folds in the intestinal mucosa (the valves of Kerckring) and villi are homologous structures, but that villi are a specialized form found most frequently in higher vertebrates such as mammals. Villus shapes may vary widely and include finger-shaped, threadlike, leaf-shaped, and wartlike. Villi measure approximately 0.5 to 1.0 mm in length and 0.2 mm in width (86). In gnotobiotic pigs the villi tend to be longer than in normal pigs (60). The total number of villi in pigs increases by 60 fold from birth to maturity (71). The lamina propria serves as the supporting area of the villus. It contains leukocytes, glands, lacteals, veins, arteries, and muscle fibers which originate from the muscularis mucosa and extend to the tip of the villus (86). These muscle fibers are responsible for the movement of the intestinal villi and contractions which cause shortening of the villi (74). The lamina propria is enclosed by the basement membrane on which the epithelial cells rest (75). The crypts of Lieberkuhn are located at the base of the villi and are a continuation of the epithelium covering the villi. They penetrate the mucosal surface and extend almost to the muscularis mucosa (9). Through serial sectioning, Cocco (20) presented the three-dimensional aspect of the crypts in relation to the villi.

### Epithelium

Three cell types make up the epithelium of the mucosa of the small intestine: columnar absorptive cells with striated borders, goblet cells, and argentaffin cells. The absorptive cells of the small

intestine are columnar to prismatic in form (9). Radioautography has been helpful in showing the continual cellular replacement that occurs in the intestine. By labeling cells with tritiated thymidine, the movement of cells in the intestine can be followed (66). Epithelial cells originate as undifferentiated cells in the crypts and move upward along the sides of the villus. At the villus apex, they reach a distinct cleft called the extrusion zone. Here they are squeezed out of position and shed into the lumen (66). As migration takes place, the crypt cells differentiate into goblet or columnar cells (9). The absorptive cells become taller during migration and the cytoplasm changes from basophilic to acidophilic. This differentiation also brings about changes in the absorptive capacity of the cell. Cells near the apex (the oldest and most differentiated) have the greatest capacity for absorption of lipids and sugars and possibly for transport of these substances into the lamina propria (66).

The time required for epithelial cell migration from the crypts to the villus tip has been calculated to be seven to ten days in one day old suckling pigs and two to four days in three week old pigs. The shorter time for the three week old pigs may be related, in part, to an increased rate of cell loss resulting from their exposure to intestinal microflora (58).

Goblet cells are found scattered among the columnar cells of the epithelium and are an example of a unicellular gland. They secrete a protein-polysaccharide called mucin which, when combined with water, forms a lubricating substance called mucus (9). This protects the intestinal surface from mechanical irritation and harmful effects of

enzymes, and aids the movement of material through the intestine (86).

Argentaffin cells are found singly, in varying numbers, scattered between cells lining the crypts of Lieberkuhn (86). These cells contain serotonin which, among other properties, is a stimulant of smooth muscle contraction (9).

### Microvilli

The surface of the epithelial cells on the villi and in the crypts consists of tiny finger-like projections known as microvilli, the brush border, or the striated border (66). Brown (15) found that the microvilli on crypt epithelium are short, broad, and relatively sparse. As the cells migrate and mature, the microvilli become longer, narrower, and more numerous. On mature cells, the average height is 1.36  $\mu\text{m}$  and the average diameter is 0.08  $\mu\text{m}$ . The microvilli increase the total absorptive area of the epithelial cell by a factor of 30 (45). A polysaccharide layer or "fuzzy coat" often covers the surface of the microvilli (39).

### ROTAVIRUSES

In 1969, Mebus et al. (48) reproduced diarrhea in calves using a virus obtained from filtered fecal material from a scouring calf. Using a fluorescent antibody specific for this virus (neonatal calf diarrhea virus or NCDV), bright fluorescence was produced in the epithelial cells of the villi of the small intestine of infected calves. The NCD virus has been successfully adapted to cell culture (49).

Characterization of the NCD virus was carried out by Welch and

Thompson (89). In morphologic characteristics and certain physical properties, the NCD virus is similiar to viruses of the Reoviridae family, which consists of the genera Reovirus and Orbivirus. However, the NCD virus has certain differences from the reoviruses. They are: 1, a decrease in infectivity when heated to 50 C in 1M MgCl<sub>2</sub>, 2, no ability to agglutinate either bovine or human erythrocytes, 3, a different cytoplasmic fluorescence than reoviruses in infected cells, and, most importantly, 4, no demonstrable reaction with reovirus antisera. The NCD virus is also acid stable which distinguishes it from the orbiviruses which are acid labile (11).

Bishop et al. (8) reported the presence of virus particles in the duodenal epithelial cells in children suffering from acute non-bacterial gastroenteritis. On the basis of morphologic characteristics, he identified these particles as orbiviruses. In 1974, Flewett et al. (29) found that on the basis of serum cross-neutralization, the viruses from diarrhetic children and calves are related. But close examination of micrographs revealed that reoviruses and orbiviruses do not possess the well defined circular outline of the human and calf gastroenteritis virus. They felt that these reovirus-like viruses should be placed in a genus separate from the Reovirus and Orbivirus and suggested the name Rotavirus (from Latin, rota=wheel). The term duovirus has also been proposed for this group (23,35) but has not been in current use. Further studies have demonstrated the presence of rotaviruses in the intestinal mucosa and fecal extracts of infants and young children with diarrhea (28,95).

In 1974, a serologic study by Woode and Bridger (90) indicated that pigs may be naturally infected with NCD virus or a similar virus. In 1976, rotavirus agents were found associated with gastroenteritis in neonatal pigs (32,92). The viruses were morphologically and antigenically similar to the rotaviruses of children and calves. However, the pig virus did not cause agglutination of human erythrocytes, which suggested that it, like the NCD virus, was not a reovirus and probably should be classified as a Rotavirus.

Rotaviruses other than the NCD virus have been difficult to culture in the past (43,73,92,94). However, recent work has shown rotaviruses to be successfully propagated by treating them with pancreatin or trypsin (4,80). Rotaviruses have also been found in lambs (43,76), antelope (72), rabbits (16,70), and foals (30).

Rotaviruses from children, calves, piglets, mice, and foals are indistinguishable from each other morphologically and share a common antigen (93). Because of their common antigenicity, cross infections may occur naturally and have been demonstrated experimentally. Gnotobiotic pigs (14,84) as well as gnotobiotic calves (53,55) have been found to be susceptible to infection by a rotavirus that caused infantile gastroenteritis. Additionally, gnotobiotic pigs are susceptible to the rotavirus of neonatal calf diarrhea (32).

fine probe and focused on the specimen by a series of electromagnetic lenses. A scanning coil deflects the beam about the specimen surface in a raster, moving back and forth until the entire surface is scanned. Secondary electrons are excited and emitted from the electron-rich surface of the specimen and accelerated into a collector where they strike a scintillator. These electrons are passed through a photomultiplier and directed into a cathode ray tube. A second scanning coil moves the transmitted beam across the visual display tube in synchrony with the raster traversing the specimen. In this way, a one-to-one point correspondence is generated between the specimen and the display. The three-dimensional effect of the image is caused by the bright-dark contrast. The variation in specimen brightness depends on the amount of electrons collected from the specimen surface, which in turn is governed by the angle of the primary beam to the specimen contour and its orientation in respect to the collector. A second display tube is used to record the image on film. By turning and tilting the specimen, it can be examined from all sides at magnifications of 20 X to 180,000 X.

#### Specimen Preparation. Fixation and Dehydration

Before SEM, specimens must first be fixed to stabilize all non-aqueous solids. This is accomplished by using formaldehyde, gluteraldehyde, osmium tetroxide, or combinations thereof. Low surface tension solvents such as ethanol, acetone, ether, 1,2-epoxypropane, or amyl acetate in graded concentrations may be substituted for water in

the tissue. However, this process produces some shrinkage (12). Maser and Trimble (46) described the use of 2,2-dimethoxypropane (DMP) as a dehydrating agent. The action of DMP is a chemical dehydration rather than a physical replacement of water with ethanol or acetone. The DMP process is more rapid and complete, and less expensive than conventional dehydration. Because the temperatures resulting from the endothermic reaction between DMP and water are lower than in the conventional method, and shorter times are involved, there is less lipid extraction and minimal solvent damage. The use of DMP may also help to eliminate shrinkage of tissues caused by ethanol or acetone in critical point drying (13).

#### Drying

Specimens may be dried directly from the solvents, but even with extremely volatile solvents such as Freon 113, shrinkage damage occurs because of surface tension. Freeze drying also causes microscopic damage caused by ice crystal formation and puncture hole artifacts (13). Presently, it seems the best way to avoid ice crystal damage and surface tension barriers is through critical point drying. In this process, the tissue, after dehydration, is permeated with a transitional fluid under pressure such as carbon dioxide ( $\text{CO}_2$ ) or various freons. When heat is applied, the temperature and pressure exceeds the transitional fluid's critical point, the temperature and pressure at which the phase boundary between liquid and gaseous  $\text{CO}_2$  (for example) vanishes and only gaseous  $\text{CO}_2$  remains. At this point, the gaseous  $\text{CO}_2$  is released without the reappearance of the liquid  $\text{CO}_2$  phase and accompanying surface tension damage. The theory and practices of critical point drying have been reviewed by Bartlett and Burstyn (6) and Cohen (21).

### Application of Metal Surface

After they are dried, it is necessary to apply a thin metal coat to soft tissues to increase thermal and electrical conductivity, enhance secondary electron emission, and increase resolution at high magnification. The metals used include silver, aluminum, gold, carbon, chromium, copper, palladium, or platinum. They are applied separately, layered, or as alloys by vacuum evaporation or sputtering (12). Specimen coating techniques have been reviewed by Ehlin (27) and DeNee and Walker (25).

An alternate method of applying a metal coat has been discussed by Kelley et al. (40) and Malick and Wilson (44). This involves the sequential binding of osmium metal, thiocarbohydrazide, and osmium metal again to the specimen surface prior to dehydration and drying. Because the thickness of the coat is only 40 to 200 Å as compared to up to 700 Å in vacuum coating (77), visualization of structures previously obscured occurs. Specimen damage from heat and mechanical vibration is also avoided.

### SCANNING ELECTRON MICROSCOPIC DESCRIPTION OF THE SMALL INTESTINE

Until the advent of the SEM, reconstruction of the structure of the small intestine had to be done by painstaking serial sectioning (20). The SEM observations of intestinal mucosa by many investigators (3,5,24,45,51,55,57,62,65,77) have helped to clarify and increase the understanding gained previously by histologic examination of this region.

Villi

In studies of human intestinal mucosa obtained through biopsy



(24,45,83), finger-shaped, tongue-shaped, leaf-shaped, and ridge forms of villi are considered normal variations. Though they sometimes are irregularly shaped, the predominant villus form in calves and pigs is finger-shaped (51,65,88). The surface of many villi is interrupted by transverse grooves running perpendicular to the villus length (3,51,65,83,88). These surface grooves can be seen in histologic preparations (45), and Demling et al. (24) have suggested that the grooves are caused either by normal contraction or by shrinkage during fixation. However, Toner and Carr (83) using the dissecting microscope were able to observe indentations in wet tissues, and doubted that they could be caused by a shrinkage artifact. Asquith et al. (3) and Marsh and Swift (45) demonstrated the arrangement of the openings of the crypts of Lieberkuhn on the intestinal floor. The tip of the villus, where cellular disintegration is evident, has been identified as the extrusion zone (3,51,65,83).

#### Epithelium

The pattern of epithelial cells is regular and hexa- or polygonal (3,5,45,83). Individual cells may be seen projecting hemispherically from the villus surface (3,24,63,83,88). Because of this hemispherical bulging, an increase of 25% in the absorptive surface area may result (24). Conversely, shrinkage and contraction of cellular cytoplasm during specimen preparation may delineate the tight cell junctions (45,83). Numerous pits on the surface of the villi correspond to the openings of individual goblet cells. They may be observed in various stages of mucus discharge (45,51,65,83).

### Microvilli

Demonstration of microvilli has been variable. Millington et al. (57) used isolated brush borders to demonstrate structures interpreted as microvilli, and Marsh and Swift (45) depicted rod-shaped microvilli. The frequent failure of most investigators to clearly resolve individual microvilli has been attributed to the "fuzzy coat," deposits of mucus, and the evaporated metal coating (3,24,83). According to Demling et al. (24), observations of microvilli structure may be of increasing importance:

"With improved fixing techniques and better coating of the surface, it should be possible to represent the microvilli too with a higher degree of accuracy. It is possible that then, or also in serious cases of malabsorption, deviations from the normal intestinal mucosa will be detected in the fine structure as well."

### OBSERVATIONS OF ROTAVIRAL INFECTIONS

The villi and the epithelial mucosa of the small intestine are affected the most following infection with rotavirus as seen by light microscopy. The lesions of gnotobiotic pigs and calves infected with rotavirus are similar (10,33,42,50,67,81,91,92). Villi become shorter, and columnar cells are replaced by cuboidal or flattened cells that often lack a brush border. Desquamation of epithelial cells results in denuded villi with exposed lamina propria. The number of reticulum-like cells increase within a thickened lamina propria.

With application of specific fluorescent antibody, immunofluoresence of epithelial cells, when present, is heaviest in the mid and lower small intestine. In gnotobiotic and conventional pigs, villi are often

fused and share their epithelium. In conventional animals the pathogenesis is enhanced by the presence of bacterial flora (50).

By SEM (42,52,54,55), villi are often observed as fused, shortened irregular in size and covered with irregular shaped epithelial cells. Exposed lamina propria is clearly visible with round to squamous shaped epithelial cells along the edges.

## MATERIALS AND METHODS

### Gnotobiotic Pigs

Fourteen pigs derived by cesarean section were kept in sterile plastic rearing isolators five days before inoculation. Two pigs were housed in each isolator unit. The inoculated pigs were maintained in the isolators until they were euthanitized for necropsy.

### Inoculum

To prepare an inoculum, fecal material was collected from pigs with clinical signs of rotaviral diarrhea. For confirmation, a direct electron microscopic examination was done on negatively stained fecal preparations (subsequently described). A 10% suspension of fecal material (w/v) in Hank's balanced salt solution was prepared and centrifuged 15 minutes at 3,000 g. The supernatant fluid was prefiltered through a 0.65  $\mu$ m millipore filter, refiltered through a 0.22  $\mu$ m millipore filter, and retained for inoculum. For negative staining, five ml of the filtrate (or 10% fecal suspension following centrifugation at 3,000 g for 15 minutes) was centrifuged 30 minutes at approximately 40,000 g. The pellet was resuspended in 20 drops of sterile, double distilled water, two drops of 4% phosphotungstic acid, pH 6.8, and one drop of 0.1% bovine serum albumin. After mixing, this suspension was sprayed onto carbon backed, collodion coated 300 mesh grids and examined on a Hitachi HU-12 electron microscope for the presence of rotavirus.

### Inoculation and Specimen Collection

In Trial 1, each of 10 pigs was inoculated orally with two ml of the fecal preparation supernatant containing rotavirus and another two

ml of the supernatant added to the ration. No method was available to determine the number of infectious particles. Pigs were euthanitized at 12 hour intervals (Table 1), and sections of the middle of the small intestine (M.I.), duodenum (Duod.), upper jejunum (U.J.), lower jejunum (L.J.), upper ileum (U.I.), and lower ileum (L.I.) were collected. The lumen of each section of intestine was rinsed with a phosphate buffered formalin solution (10%) and then filled with the solution and submerged in a container of the formalin solution for fixation.

In Trial 2, six pigs were inoculated with a virus suspension prepared as previously described from fecal material collected during the early scouring stages of pigs in Trial 1. Inoculation procedures were the same as for Trial 1. Pigs were euthanitized at 24 hour intervals beginning at 24 hours and ending at 144 hours following inoculation along with control pigs at 48 and 120 hours.

#### Light Microscopic Examination

Formalin fixed tissues were embedded in paraffin, sectioned 6  $\mu$ m thick, and stained with hemotoxylin and eosin according to accepted procedures.

#### Scanning Electron Microscopic Examination

For SEM, small (approximately  $0.5 \text{ cm}^2$ ) pieces of tissue were excised from the formalin fixed intestinal segments and placed villus side up in small glass vials. The specimens were rinsed eight hours in each of three changes of 5% gluteraldehyde in 0.2 M phosphate buffer, pH 7.4, at room temperature. Specimens were then washed eight hours in each of three changes of double distilled water at room temperature.

Table 1. Number of the pigs and time after exposure the pig was euthanatized.

<u>Pig #</u>	<u>Treatment</u>	<u>Hours after exposure</u>
AAJ-1	Virus	12 Hours
AAJ-2	Virus	24 Hours
AAJ-3	Virus	36 Hours
AAJ-4	Virus	48 Hours
AAJ-5	Virus	60 Hours
AAJ-6	Virus	72 Hours
AAJ-7	Virus	84 Hours
AAJ-8	Virus	96 Hours
AAJ-9	Virus	Hyperantiserum
AAJ-10	Virus	Hyperantiserum
AAJ-11	Control	24 Hours
AAJ-12	Control	72 Hours
AAJ-13	Control	96 Hours
AAJ-14	Control	48 Hours

A 1% solution of  $\text{OsO}_4$  was prepared by adding 1 gram of  $\text{OsO}_4$  to 100 ml of double distilled water. The solution was not used until all  $\text{OsO}_4$  crystals had dissolved (approximately 24 hours). A saturated solution of thiocarbohydrazide (TCH)<sup>1</sup> was prepared fresh before each processing procedure by adding approximately 0.1 grams of TCH to 100 ml of double distilled water and heating in a hot water bath (50-60 C) for 45 minutes with occasional agitation. The solution was filtered through a 0.45 um millipore filter to remove undissolved TCH crystals.

Sequential binding of  $\text{OsO}_4$  and TCH to the tissues was accomplished by slightly modifying the procedure of Malick and Wilson (44) as follows:

Step 1. Apply 1%  $\text{OsO}_4$  to tissues for 30 minutes at room temperature.

Step 2. Rinse tissues in three changes of double distilled water over 30 minutes at room temperature.

Step 3. Apply saturated TCH solution to tissues for 30 minutes at room temperature.

Step 4. Repeat steps 2, 1, 2, 3, 2, 1, 2.

The resultant binding sequence to the tissues is  $\text{OsO}_4$ -TCH- $\text{OsO}_4$ -TCH- $\text{OsO}_4$ .

To dehydrate the tissues, acidified 2,2-dimethoxypropane (DMP)<sup>2</sup> (1 drop conc. HCl per 50 ml DMP) was applied according to the method of Maser and trimble (46) except that only two ml of acidified was applied for 15 minutes at room temperature. The DMP was removed and

---

<sup>1</sup>Polysciences, Inc., Warrington, PA.

<sup>2</sup>Polysciences, Inc., Warrington, PA.

two ml of 100% ethanol applied for 15 minutes.

To dry the tissues, the dehydrated, ethanol-treated tissues were placed in three small wire baskets, each with a small metal piece dividing the basket into two sections. In this way, six tissues could be dried at a time. The baskets were placed in the drying chamber of a critical point drying apparatus<sup>1</sup> filled with 100% ethanol and dried using liquid CO<sub>2</sub> according to the method of Anderson (2). Liquid CO<sub>2</sub> was slowly introduced into the chamber through the chamber inlet valve. With the inlet valve open, the chamber exit valve was opened slightly for five minutes, allowing the ethanol to escape, and then closed for ten minutes. During this procedure, the pressure was maintained at 800-1,000 p.s.i. This procedure was repeated until no ethanol could be detected leaving the chamber. The inlet valve and exit valve were then closed and a large plastic beaker of hot water (50-60 C) placed around the drying chamber. The pressure increased and was maintained at 1,500 p.s.i. for ten minutes. The exit valve was then opened slightly to allow the vaporized CO<sub>2</sub> to escape at a rate of 100 p.s.i. for 15 minutes. The drying chamber remained in the hot water bath until the venting was complete. The dried specimens were attached with silver conducting paint<sup>2</sup> to 3/8" aluminum SEM studs<sup>3</sup> and examined on a JEOL JSM-35 SEM operated at an accelerating voltage of 25 KV and at a

---

<sup>1</sup>Denton Vacuum, Inc., Cherry Hill, NJ.

<sup>2</sup>Acme Chemicals and Insulation Co. (Division of Allied Products Corp.), New Haven, CT.

<sup>3</sup>Ladd Research Industries, Inc., Burlington, VT.



working distance of 39 mm except where noted. Images were recorded on black and white film<sup>1</sup> with a scan rate of 3,000 lines/frame.

---

<sup>1</sup>Polaroid P/N 55, Polaroid Corp., Cambridge, MA.

## RESULTS

### TRIAL 1

Results of the scanning electron microscopic examination are presented in Table 2. Those features which could be evaluated, such as rounding of epithelial cells on the villus surface, exposure of the lamina propria, and villus fusion, are shown. The data presented in the table represents the changes noted in intestinal appearance. Scanning electron micrographs supplemented with light micrographs and appropriate controls will be discussed by 12 hour intervals to illustrate the development, type, severity, and location of the lesions observed.

#### 12 Hours

In the upper and lower jejunum and mid intestine, the ends of the villi were contracted, forming pyramidal shaped tips. Sporadic villi were bifid and had deeply indented extrusion zones forming two distinct areas on the ends of the villi. Transverse ridges and goblet cells were readily visible (Fig. 1) just as they were on the control tissues, where villi were long, slender, and of varying lengths, with goblet cells being empty or discharging mucus (Fig. 2). The upper ileum villi were similiar in appearance to villi in the mid intestine. By LM, villi of the infected lower jejunum were long and slender, occasionally showing a contracted lamina propria and pyramidal shaped villus tips although villi did not appear contracted (Fig. 3). Control villi of the lower jejunum were long and finger-like with vacuolation present in epithelial cells on the distal half of the villi (Fig. 4).

Villi in the lower ileum changed markedly in appearance from that

Table 2. Scanning Electron Microscopic Findings in the Intestines of Rotavirus Infected Gnotobiotic Piglets

Villus Morphology				Villus Morphology			
	Absorptive Cell Rounding	Exposure of Lamina Propria	Villus Fusion		Absorptive Cell Rounding	Exposure of Lamina Propria	Villus Fusion
12 hrs.				60 hrs.			
Duod.	-	-	1	Duod.	-	-	1
U.J.	-	-	-	U.J.	-	-	-
L.J.	-	-	1	L.J.	+	-	-
M.I.	-	-	-	M.I.	+	-	2
U.I.	-	-	-	U.I.	+	1	2
L.I.	++	-	-	L.I.	-	-	-
24 hrs.				72 hrs.			
Duod.	-	-	-	Duod.	-	-	1
U.J.	+	-	-	U.J.	+	2	4
L.J.	+	-	-	L.J.	+	2	4
M.I.	+	1	-	M.I.	+	2	4
U.I.	+	-	-	U.I.	+	3	3
L.I.	++	1	-	L.I.	-	-	-
36 hrs.				84 hrs.			
Duod.	-	-	3	Duod.	+	-	1
U.J.	+	-	1	U.J.	+	2	4
L.J.	+	-	-	L.J.	+	4	4
M.I.	+	1	-	M.I.	-	4	4
U.I.	-	-	-	U.I.	-	3	2
L.I.	-	-	-	L.I.	-	-	-
48 hrs.				96 hrs.			
Duod.	-	-	-	Duod.	+	-	2
U.J.	-	-	-	U.J.	+	-	4
L.J.	-	-	-	L.J.	+	1	4
M.I.	+	1	-	M.I.	-	1	4
U.I.	+	1	1	U.I.	-	1	4
L.I.	-	-	-	L.I.	-	-	-

\*Rounding of epithelial cells in the lower ileum explained in the Discussion.

Absorptive Cell Rounding  
 Irregular-sized clusters or individual epithelial cells rounding up on villi tips, sides, and/or edge of lamina propria exposure (where applicable)  
 - Rounding absent  
 + Rounding present

Lamina Propria Exposure  
 - No exposure of L.P.  
 1 L.P. exposed on isolated villi or villus clusters  
 2 L.P. exposed on approx. 25% of villi or villus clusters  
 3 L.P. exposed on approx. 25-75% of villi or villus clusters  
 4 L.P. exposed on approx. 75-100% of villus clusters

Villus Fusion  
 - No fusion seen  
 1 Pairs or groups of villi fused in isolated areas  
 2 Approximately 25-50% of villi fused in pairs or groups  
 3 Approximately 50-75% of villi fused in pairs or clusters  
 4 Approximately 75-100% of villi fused in pairs or clusters

of the upper intestine. Very large, ballooning epithelial cells covered the entire villus surface and villi appeared shorter and broader. Rounded epithelial cells on the sides and tips of the villi showed a darkened surface caused by the loss of microvilli on the cell surface (Fig. 5). The control lower ileum villi also had prominent epithelial cells covering the surface of the villi, although in a much more regular fashion, and the villi were not contracted (Fig. 6). Light microscopic examination of the lower ileum showed the epithelial cells to be vacuolated along the length of the villi with occasional exposure of the lamina propria (Fig. 7). Control villi were long and slender by LM (Fig. 8). Vacuolation of the control villus epithelium increased when progressing distally through the small intestine with the heaviest vacuolation toward the tips of the villi (Figs. 4,8).



Figure 1. Scanning electron micrograph of the lower jejunum 12 hours post inoculation (PI). Most villi have pyramidal tips (P), and occasional villi have bifid tips (B). Transverse furrows are evident (T) as well as goblet cells (arrow). Extrusion zones (E) are visible on the villus tips. X 120.

Figure 2. Scanning electron micrograph of the control lower jejunum at 24 hours. Villi are long and slender and of varying lengths with rounded tips and transverse furrows (T). Goblet cells (arrows) can be seen empty or discharging mucus. X 100.

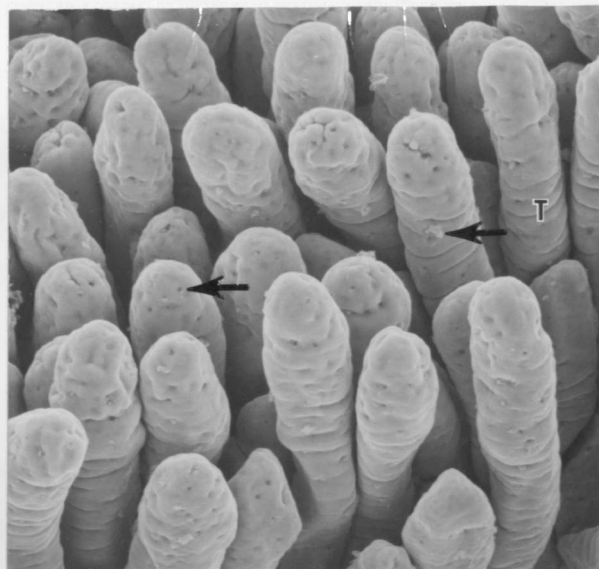
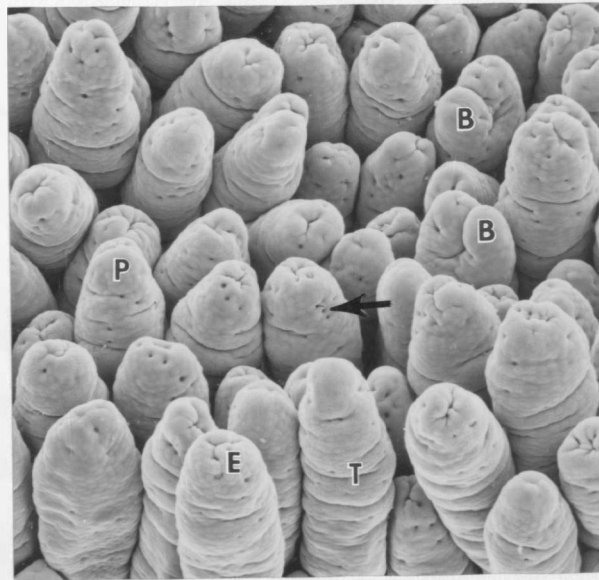


Figure 3. Light micrograph of the lower jejunum 12 hours PI. No shortening of the villi is evident. One villus has a contracted lamina propria (L) at the tip, separated from the epithelial cell layer (E). Transverse grooves are visible along the lateral edges (\*), along with some vacuolation (arrow). X 116.

Figure 4. Light micrograph of the control lower jejunum at 24 hours. Villi show the normal, slender configuration. Vacuolation is more distinct although it covers only the distal half of the villi (between arrows). X 116.

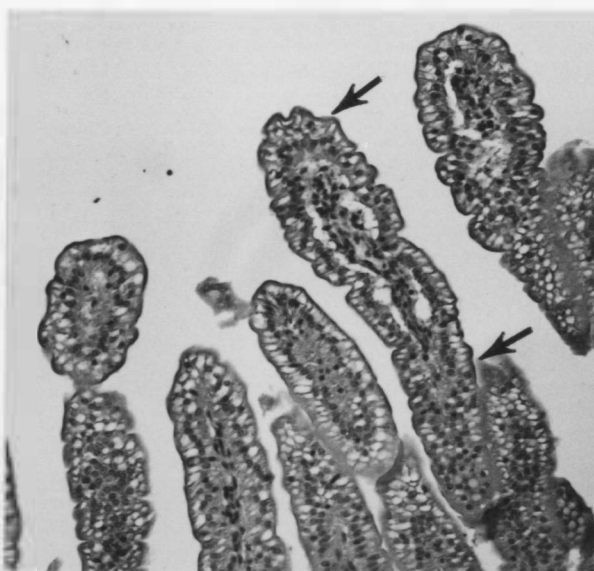
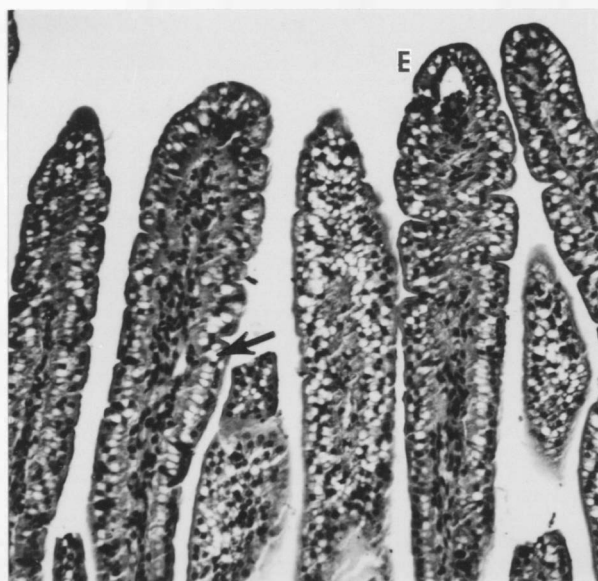




Figure 5. Scanning electron micrograph of the lower ileum 12 hours PI showing broad, contracted villi. Epithelial cells on the entire villus surface are irregularly shaped and prominent. Surfaces of some cells (arrows) on the villi tips and sides show a darkening caused by the lack of microvilli on the cell surface. X 160.

Figure 6. Scanning electron micrograph of a single lower ileum villus from the 24 hour control pig. Prominent, regular, individual epithelial cells are clearly seen protruding hemispherically into the intestinal lumen (L). X 360.

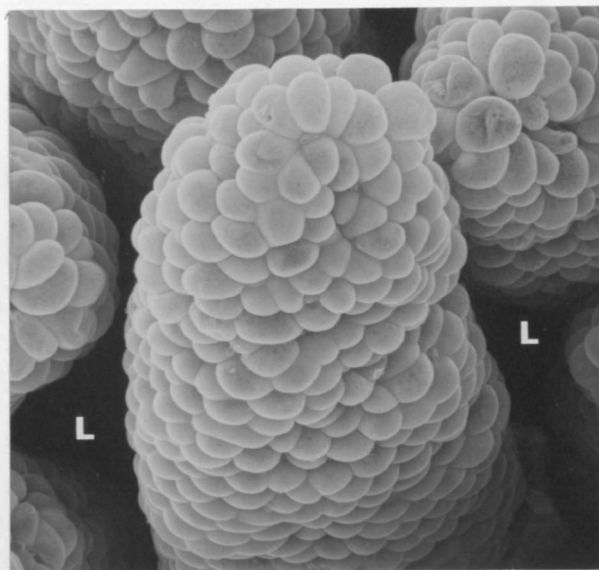
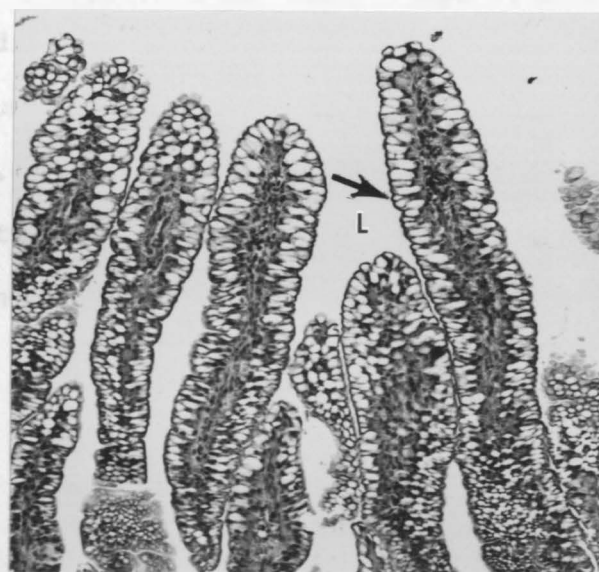
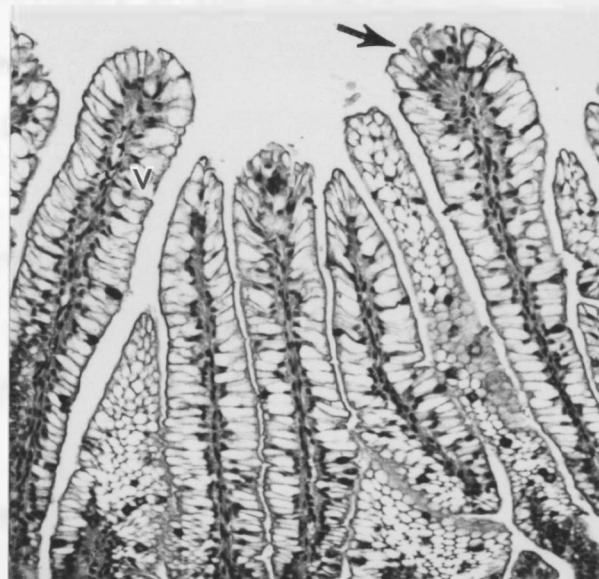


Figure 7. Light micrograph of the lower ileum 12 hours PI. Notice the extensive vacuolation (V) along the length of the villi. Some villi appear to have degenerating epithelial cells at the extrusion zone (arrow). X 125.

Figure 8. Light micrograph of the control lower ileum at 24 hours. Villi are long and slender and epithelial cells are heavily vacuolated (V) along the entire lateral edge of the villi. Epithelial cells (arrow) can be seen protruding into the lumen (L). Compare to Fig. 4. X 100.



#### 24 Hours

The first significant change caused by the rotavirus infection was the increasing prominence of the epithelial cells, especially in the lower jejunum. These cells were irregular in size and shape and covered the tips of the villi (Fig. 9). Histologic preparations also showed bulging, abnormal arrangements and piling up of epithelial cells (Fig. 10). In contrast, villi in the duodenum were very smooth and flat, almost void of all surface features except the extrusion zone and a few goblet cells (Fig. 11). Although rounding of epithelial cells was not as severe in the mid intestine and upper ileum, some villi had mild exposure of the lamina propria. A wall of tissue extended the length of several sections (approximately 4.0 mm) taken from the mid intestine (Fig. 12). Many villi in the lower ileum were visibly contracted while those that were not had varying degrees of lamina propria exposure and rounding of epithelial cells (Fig 13). Villi in the control lower ileum were long with regularly prominent epithelial cells (Fig. 14). By LM, villi in the lower ileum were short and sparse with a lack of vacuolation (Fig. 15) whereas control villi were lengthy, closely packed, and vacuolated along the entire length of the villi (Fig. 8).

Figure 9. Scanning electron micrograph of the lower jejunum 24 hours PI. Epithelial cells (E) on the tips of the villi are rounded, prominent, and irregular in size. Compare to Fig. 2. X 160.

Figure 10. Light micrograph of a single villus in the lower jejunum 24 hours PI. A single row of columnar epithelial cells is present on the lateral edges of the villi although the location of cellular nuclei (arrows) shows an abnormal arrangement of epithelial cells at the villus tip. The lamina propria (L) has contracted causing large indentations (I) in the villus surface. X 435.

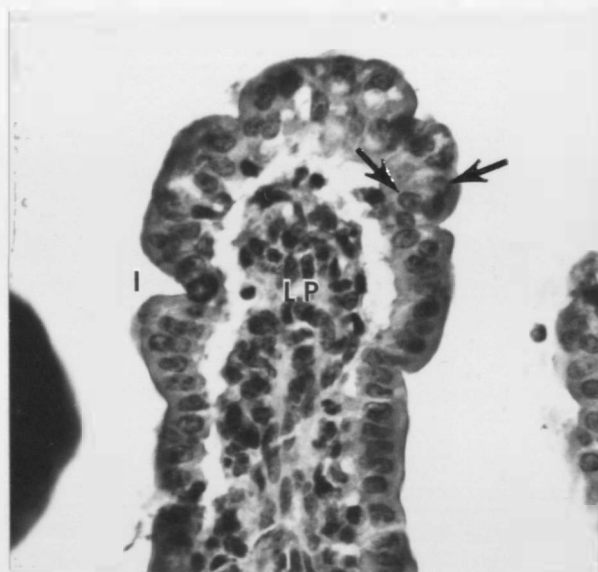
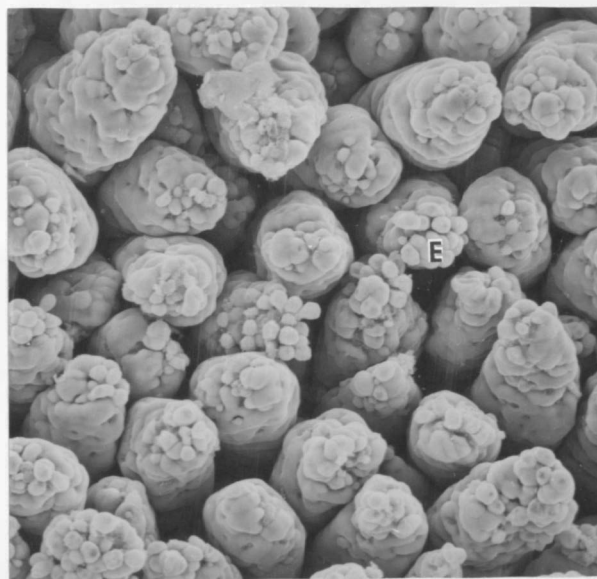


Figure 11. Scanning electron micrograph of the duodenum 24 hours PI. The villus surface is smooth and relatively uninterrupted. Extrusion zones (E) are visible on some of the villi tips as well as occasional goblet cells (arrow) on the the villus surface. X 150.

Figure 12. Scanning electron micrograph of the mid intestine 24 hours PI. A long ridge of uncertain origin runs the length of the intestinal segment (approximately 4.0 mm). Surrounding villi show exposure of the lamina propria (arrows). X 160.



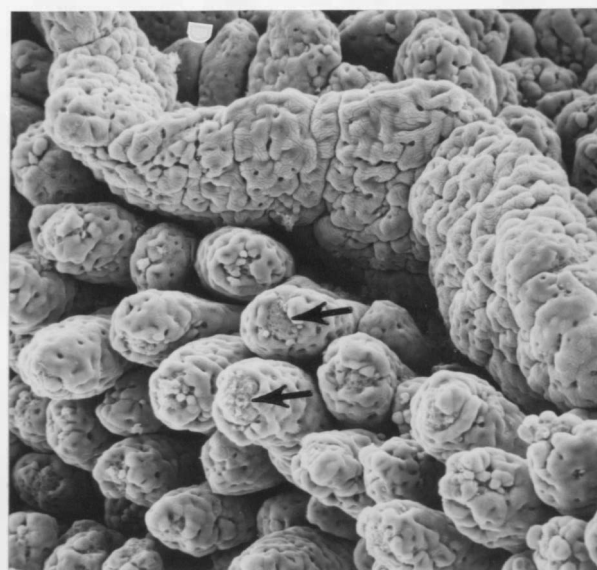
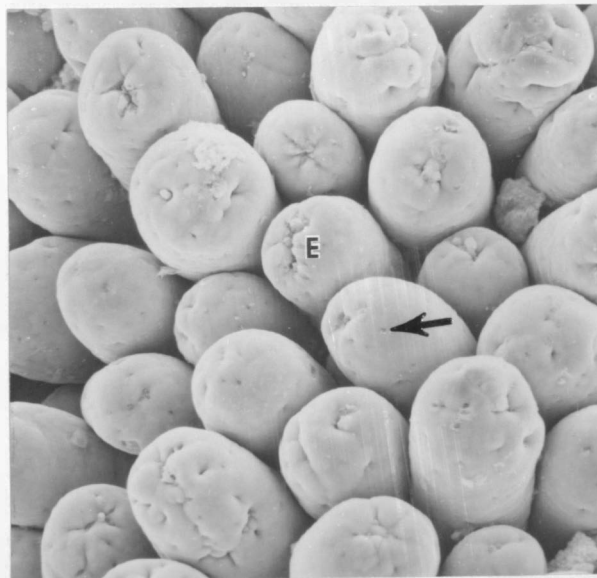


Figure 13. Scanning electron micrograph of the lower ileum 24 hours PI. Some villi are noticeable contracted (C) while those that are not show varying degrees of lamina propria exposure with rounded, prominent epithelial cells (arrows) on the villus tips. The intestinal floor (F) is easily visible between the shortened villi. Compare to Fig. 14. X 130.

Figure 14. Scanning electron micrograph of the control lower ileum at 24 hours. Villi vary in length with epithelial cells being consistently prominent on the villus surface. X 100.

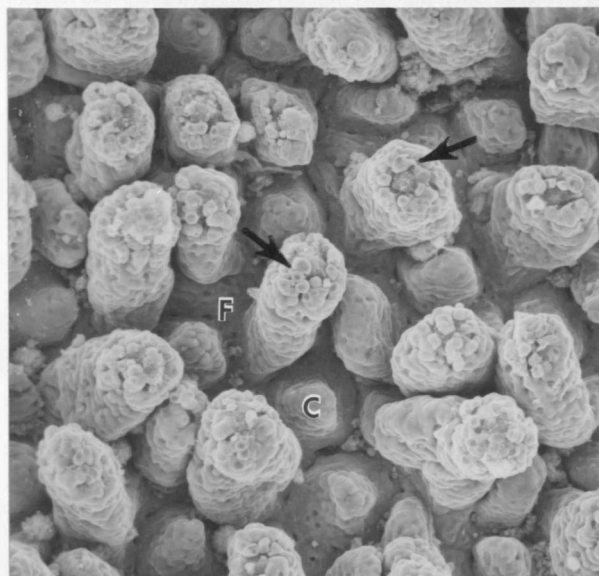


Figure 15. Light micrograph of the lower ileum 24 hours PI. Villi are shorter and fewer in number. Notice the lack of vacuolation. Compare to Fig. 8. X 122.

Fig. 100

Fig. 100. A section of the skin of a mouse, showing the epidermis and dermis. The epidermis is the outer layer, and the dermis is the inner layer. The epidermis is composed of several layers of cells, and the dermis is composed of a layer of connective tissue. The epidermis is shown as a dark, wavy line, and the dermis is shown as a lighter, more uniform area. The epidermis is shown as a dark, wavy line, and the dermis is shown as a lighter, more uniform area.

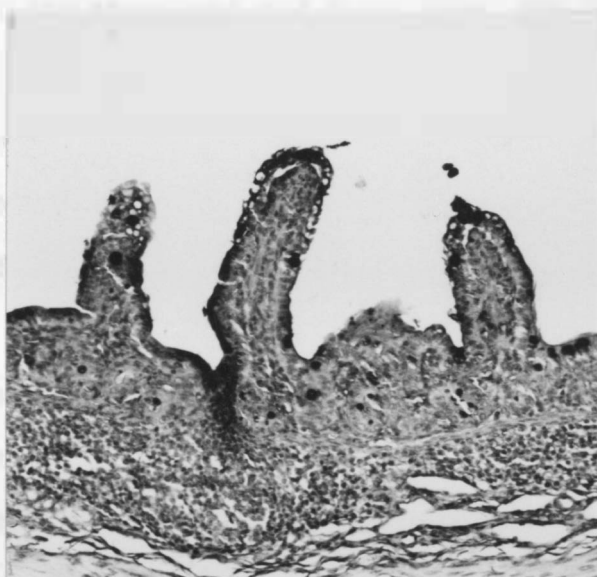


Fig. 101

### 36 Hours

Villus atrophy in the duodenum was most extensive 36 hours after inoculation. The villi were shorter with broader bases and fused to form irregular pairs and clusters. Epithelial cells and cell clusters protrude from the sides of the fused villi (Fig. 16). Many of these protruding epithelial cells exhibited reduced numbers of microvilli. In control duodenum tissues, villi were long and slender and had a smooth epithelial cell surface (Fig. 17). By LM, villi in the infected duodenum were markedly shortened and fused (Fig. 18) as compared to the long, slender villi of the control duodenum (Fig. 19). By SEM, the extent of rounding and lamina propria exposure changed little from the duodeunum through the upper ileum. By LM, the villi were shortened and occasionally fused. The lower ileum villi appeared to have recovered nearly completely as observed by SEM (Fig. 20) and remained that way through 96 hours after infection. However, the villi did not retain the regular, prominent cells of the control lower ileum (Fig. 14). By LM, villi in the lower ileum did not have exposed lamina propria or exhibit fusion (Fig. 21) but were fewer and not as long as control lower ileum villi (Fig. 8).

Figure 16. Scanning electron micrograph of the duodenum 36 hours PI. Villi are fused to form irregular pairs and clusters. Rounded epithelial cells (arrows) are visible on the tips and sides of the fused villi. Compare to Fig. 17. X 150.

Figure 17. Scanning electron micrograph of the control duodenum at 24 hours. Varying amounts of mucus and/or proteinaceous material (arrows) are present between the smooth, long villi. X 160.

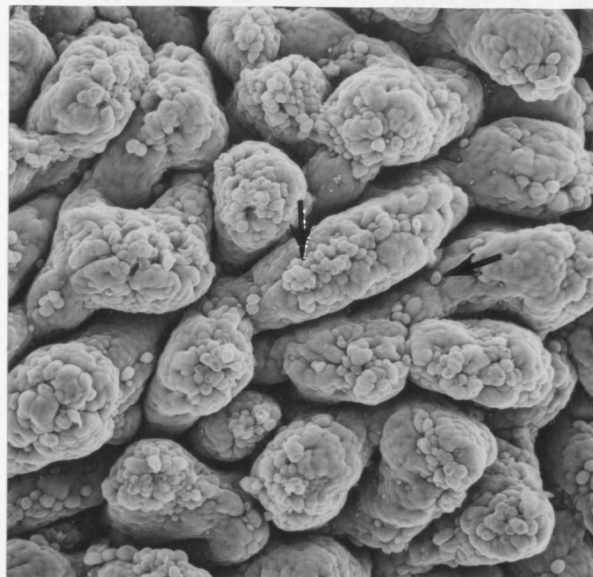




Figure 18. Light micrograph of the duodenum 36 hours PI. Villi are noticeably contracted and fused. Epithelial cells (arrows) on the ends of some villi and villus clusters are detaching and sloughing into the lumen. The longitudinal (L) and circular (C) muscle layers composing the outer layers of the intestine are visible. Compare to Fig. 19. X 160.

Figure 19. Light micrograph of the control duodenum at 24 hours. The normal, long nature of the villi is evident with a regular arrangement of columnar epithelial cells (arrow). X 105.

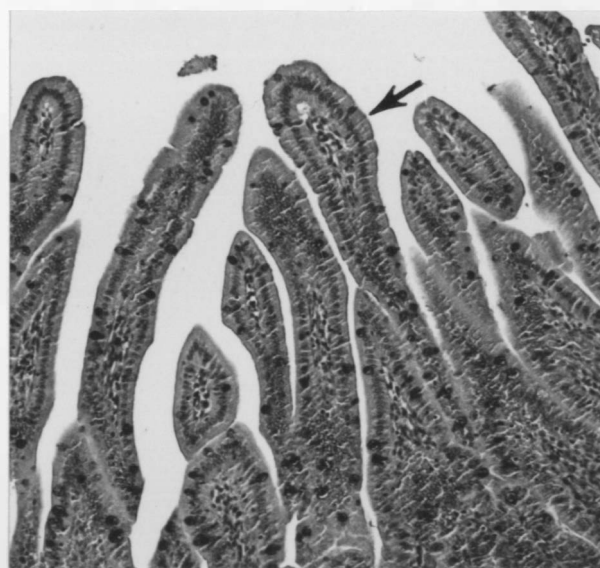
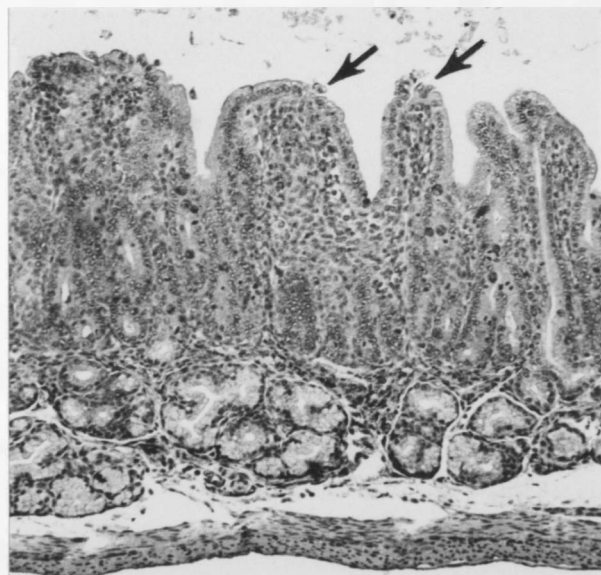
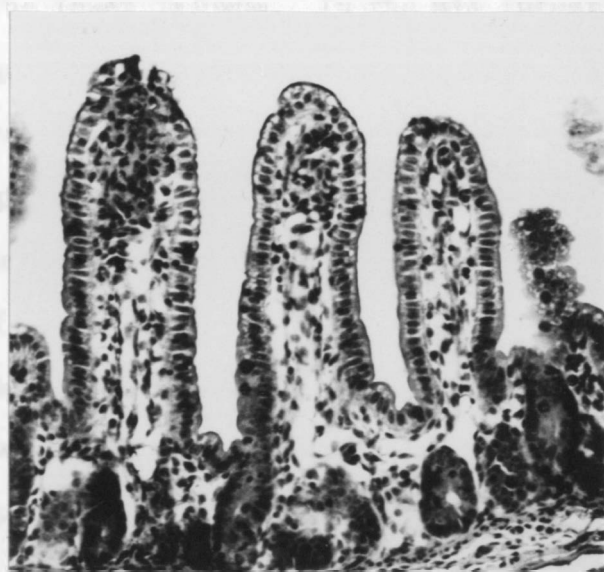
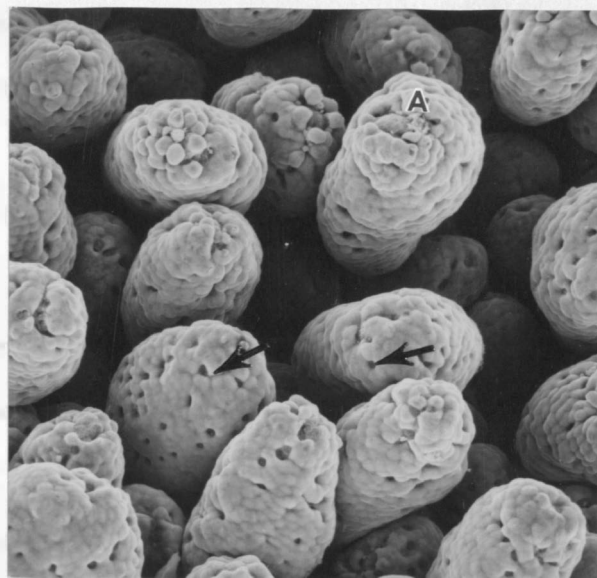


Figure 20. Scanning electron micrograph of the lower ileum 36 hours PI. Shortening of the villi is not as evident as at 24 hours PI. Villi have regained a more uniform epithelial cell surface although some lamina propria exposure is still evident (A). Goblet cells (arrows) are visible on the villus surface. Compare to Fig. 13 and 14. X 160.

Figure 21. Light micrograph of the lower ileum 36 hours PI. Villi are not affected by fusion or lamina propria exposure but are shorter and fewer than the control villi. Compare to Fig. 8. X 170.



48 Hours

Prominence of rounded epithelial cells and fusion was reduced in the duodenum through the lower jejunum. Many villi lacked the transverse grooves of the control villi and had instead many smaller, irregular grooves giving the villus surface a rough appearance. Villi in the mid intestine and upper ileum were shorter, often exposing the intestinal floor, and occasional villi were denuded at the tips exposing the lamina propria. Cells along the receding epithelial cell layer were rounded (Figs. 22,24). By LM, many villi had a contracted lamina propria with a complete, but detached, cuboidal epithelial cell layer (Fig. 23). The lower ileum remained unaffected.

60 Hours

Some fusion was evident in the duodenum, although changes were limited through the lower jejunum. In the mid intestine and upper ileum, fusion began to increase, seemingly limited to pairs of villi only. Fused villus pairs had irregularly shaped epithelial cells protruding from the sides and tips of the villi. If fusion was not evident, villi were very short and blunt so that the intestinal floor and the crypts of Lieberkuhn were visible (Fig. 25). Fusion, exposure of the lamina propria, or villus shortening was not observed in the lower ileum although prominent epithelial cells were not present on the villus surface.

Figure 22. Scanning electron micrograph of the mid intestine 48 hours PI showing shortened villi, exposed lamina propria (L), rounded epithelial cells (arrows), and exposure of the intestinal floor (F). Transverse grooves have been replaced by smaller, irregular grooves. X 270.

Figure 23. Light micrograph of a mid intestinal villus 48 hours PI with a contracted lamina propria (LP) and a detached, cuboidal epithelial cell layer (arrow). X 370.

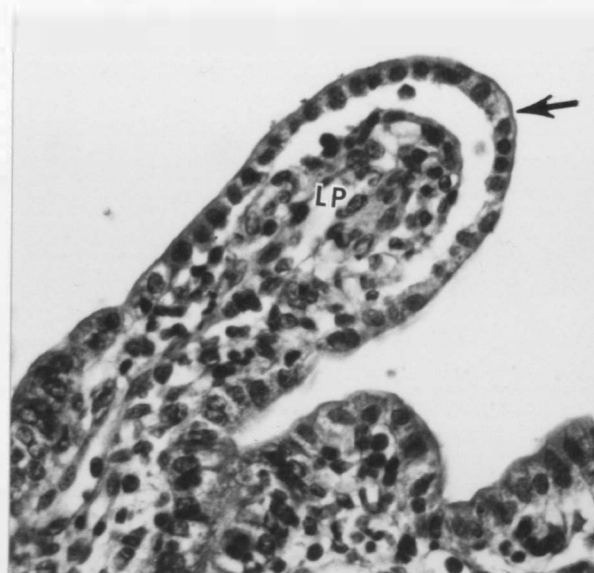


Figure 24. Scanning electron micrograph of the upper ileum 48 hours PI. Villus atrophy is apparent by the shortened, denuded villi. The epithelial cells sloughing off the villi are rounded (arrow). Transverse furrows have been replaced by irregular grooves (G) on the villus surface. Lamina propria (L), intestinal floor (F). X 240.

Figure 25. Scanning electron micrograph of the mid intestine 60 hours PI. Short, blunt villi have irregularly shaped epithelial cells at the extrusion zones (E). The crypts of Lieberkuhn are visible between the villus stumps (arrow). X 200.





### 72 Hours

Villus atrophy was most severe at 72 hours following inoculation. With the exception of the duodenum and lower ileum, all sections of the intestine were affected. In the upper jejunum, large areas of villi were fused and shared a common epithelial cell covering with most villus clusters showing extensive exposure of the lamina propria. The intestinal floor could be seen between the fused villi (Fig. 26). Contrasting this were the long, slender, upper jejunum control villi corrugated by many transverse grooves (Fig. 27). The avillus intestinal surface seen by SEM in infected upper jejunum tissues was also visible by light microscopy (Fig. 28). Likewise, histologic sections of the control jejunum verified the lengthy, individual nature of the normal villi (Fig. 29). In the mid intestine, fusion was not as severe as in the jejunum, although denuding of villi was quite widespread with epithelial cells rounded and prominent near the exposed lamina propria (Fig. 30). Because of the shortened and fused villi, it was often possible to observe red blood cells on the intestinal floor and within the openings of the crypts of Lieberkuhn (Fig. 31). Rounded epithelial cells at the edge of the exposed lamina propria or on the sides of villi or villus clusters often showed a thinning of the microvilli on the cell surface (Fig. 32,33). Microvilli on control tissues were arranged in a closely packed array (Fig. 34). Fusion and lamina propria exposure did not affect the lower ileum (Fig. 35) although it did not retain the regular, evenly prominent epithelial cells of the control villus surface (Fig. 36).

Figure 26. Scanning electron micrograph of the upper jejunum 72 hours PI. Villus fusion is 100%. Lamina propria (L) exposure is severe. Crypts of Lieberkuhn (arrow) are visible on the intestinal floor. Compare with Fig. 27. X 180.

Figure 27. Scanning electron micrograph of normal jejunal villi at 72 hours. Transverse furrows (T) are present on the length of the villi and goblet cells (arrows) are prominent at the villus tips. The intestinal floor is not visible. X 120.

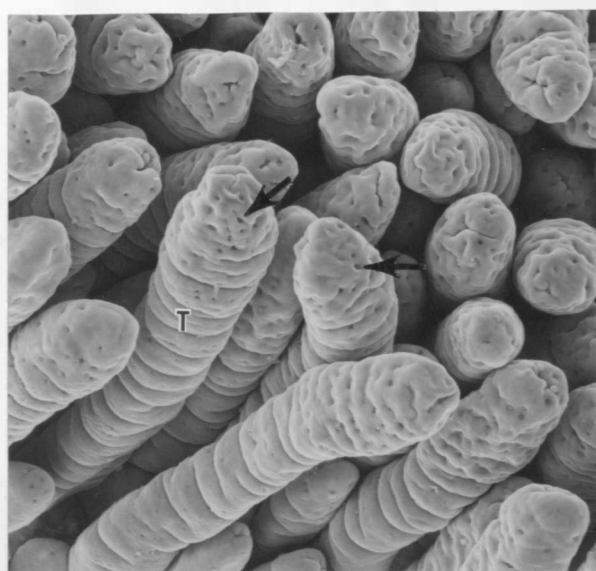
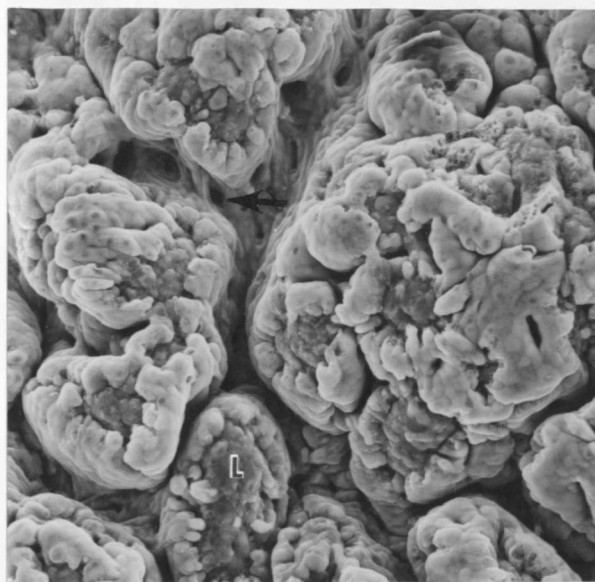


Figure 28. Light micrograph of the upper jejunum 72 hours PI. Villi are fused, flattened, and nonexistent. Crypts of Lieberkuhn (C). Compare to Fig. 29. X 150.

Figure 29. Light micrograph of the control upper jejunum at 72 hours. Villi are long and slender with many transverse grooves (\*) and dark goblet cells (arrows). X 117.

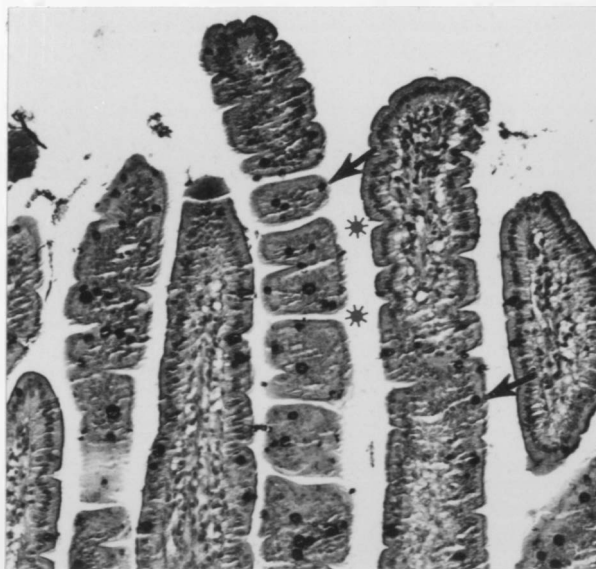
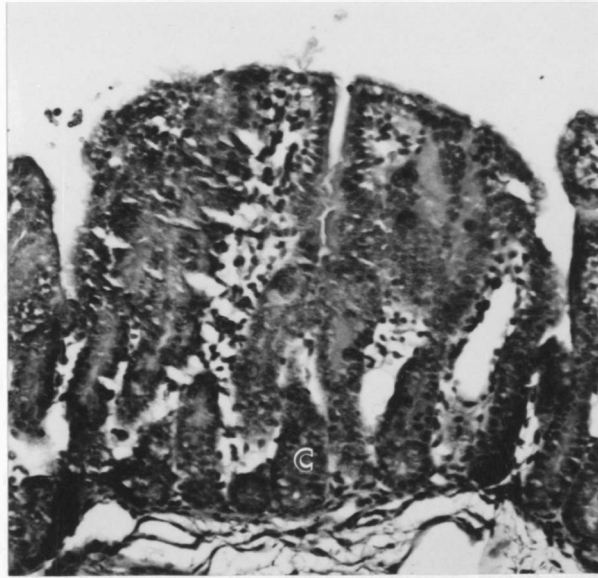


Figure 30. Scanning electron micrograph of the mid intestine 72 hours PI showing more individualized villi but with marked lamina propria exposure (L). Epithelial cells (arrow) are rounded and the crypts of Lieberkuhn are visible on the intestinal floor (C). Compare to Fig. 49. X 150.

Figure 31. Scanning electron micrograph of the upper ileum 72 hours PI. Fused villi are evident (F) and numerous red blood cells are visible on the intestinal floor and within the crypts of Lieberkuhn (arrows). X 180.

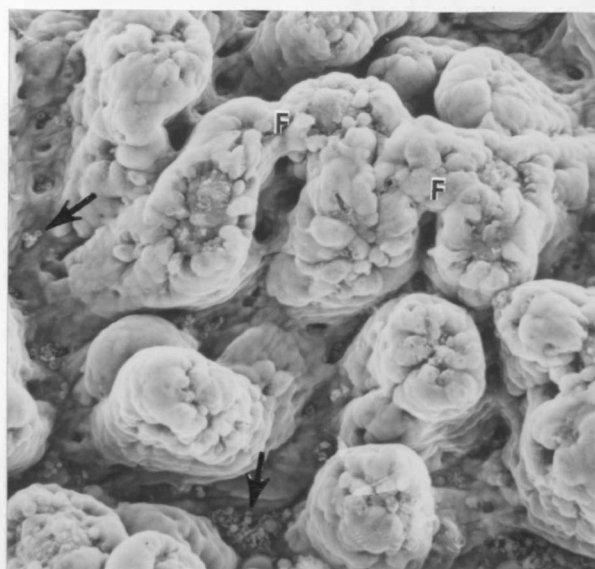
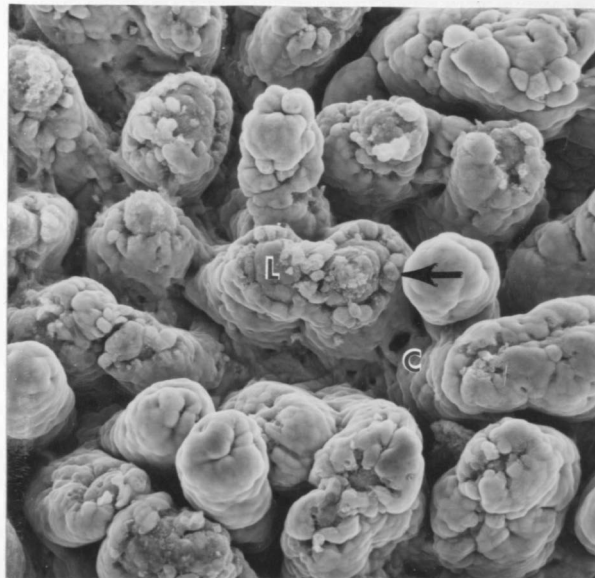




Figure 32. Scanning electron micrograph from the upper ileum 72 hours PI of a rounded epithelial cell at the edge of the exposed lamina propria (LP). An area of thinning microvilli (A) lies adjacent to an area of unaffected microvilli. Compare to Fig. 34. X 2,400.

Figure 33. Scanning electron micrograph of a rounded epithelial cell on the side of a villi in the upper ileum 72 hours PI. The entire cell surface has fewer microvilli (MV). Microvilli can be seen extending outward from the cell surface (arrow). The cell junction with a neighboring cell is visible (CJ). Compare to Fig. 34. X 4,800.

Figure 34. Scanning electron micrograph of control microvilli. Microvilli are numerous and in a closely packed array. Working distance 15 mm. Accelerating voltage 30 KV. X 18,000.

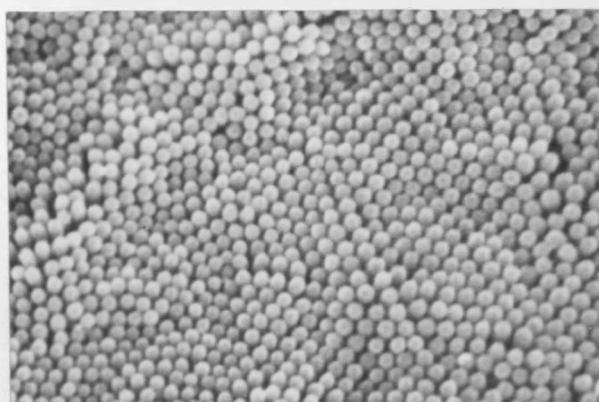
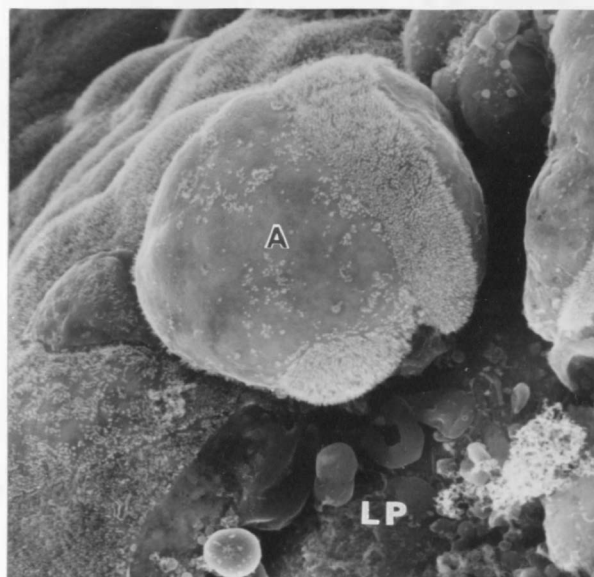


Figure 35. Scanning electron micrograph of the lower ileum 72 hours PI. Villi retain an essentially normal appearance. Transverse furrows (T) and goblet cells (arrows) on the villus tips are visible. Compare to Fig. 36. X 160.

Figure 36. Scanning electron micrograph of control lower ileum villi at 72 hours. Epithelial cells are prominent on the villus surface. Cellular degeneration is taking place at the extrusion zone (E). A few cells appear collapsed from either normal or preparative processes (arrow). X 110.

# Fig. 10

The surface of the ...

... the ...

... the ...

... the ...

... the ...

... the ...

... the ...

... the ...

... the ...

... the ...

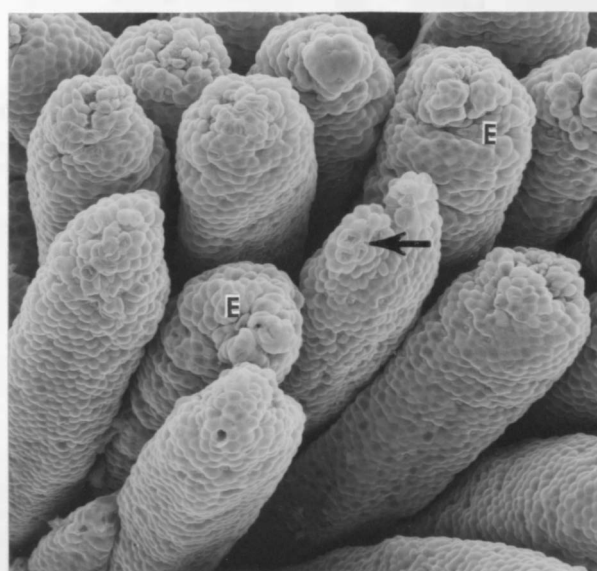
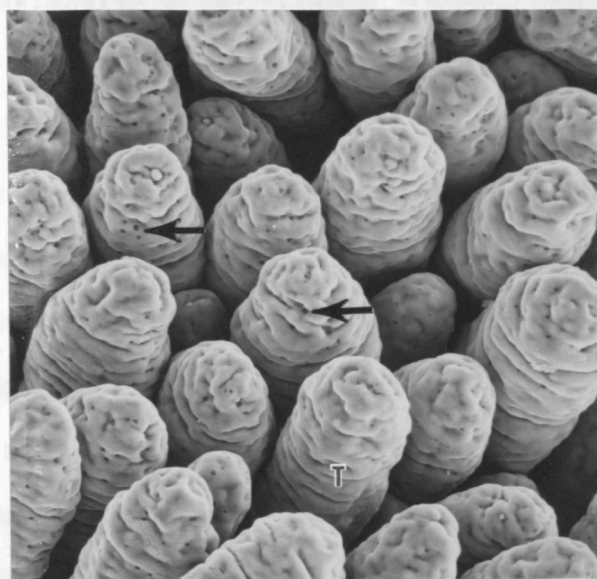
... the ...

... the ...

... the ...

... the ...

... the ...



84 Hours

The villus surface in the duodenum was rough and irregular with villus fusion occasionally noted between blunted villi (Fig. 37). Fused and denuded villi were still visible in the jejunum (Fig. 38). By LM, jejunal villi were lengthening but exposed lamina propria and shared epithelium between villi was apparent. The crypts of Lieberkuhn had increased in length by a factor of 1.5 to 2.0 as compared to the control tissues (Fig. 39). In the mid intestine, the distinctive rounding of the epithelial cells around exposed lamina propria has been replaced by more normal columnar shaped epithelial cells (Fig. 40). Although lamina propria exposure was still severe in the upper ileum, villi were more individual and epithelial cells exhibited an increased columnar appearance (Fig. 41). Control upper ileum tissues had irregularly shaped villi, varying degrees of epithelial cell prominence, and an occasional villus with an incomplete epithelial cell covering over the extrusion zone (Fig. 42).

Figure 37. Scanning electron micrograph of the duodenum 84 hours PI. The villus surface is roughened because of large wrinkles and irregular buldging of epithelial cells. Fusion is occasionally evident between blunted villi (arrow). Compare to Fig. 17. X 180.

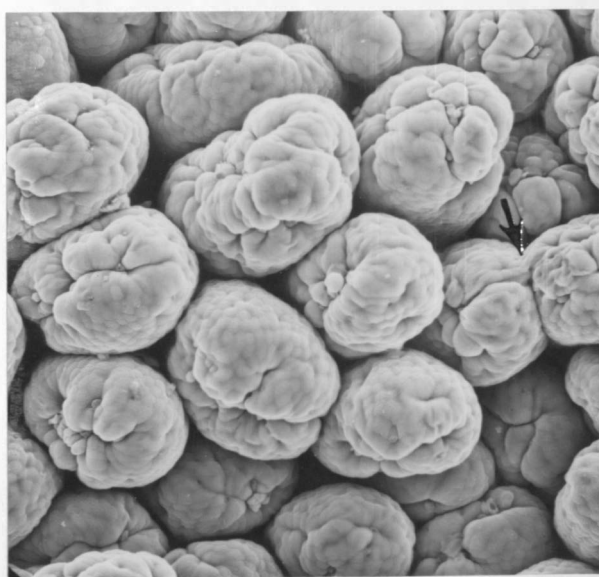


Figure 38. Scanning electron micrograph of the lower jejunum 84 hours PI. Severe fusion is evident. Adjacent to the exposed lamina propria are rounded epithelial cells (arrow). X 180.

Figure 39. Light micrograph of the lower jejunum 84 hours PI. Villi are shortened and fused (arrow) with one villus lacking a complete epithelial cell layer resulting in exposed lamina propria (A). The Crypts of Lieberkuhn are hyperplastic and have increased in length (between bars). X 121.



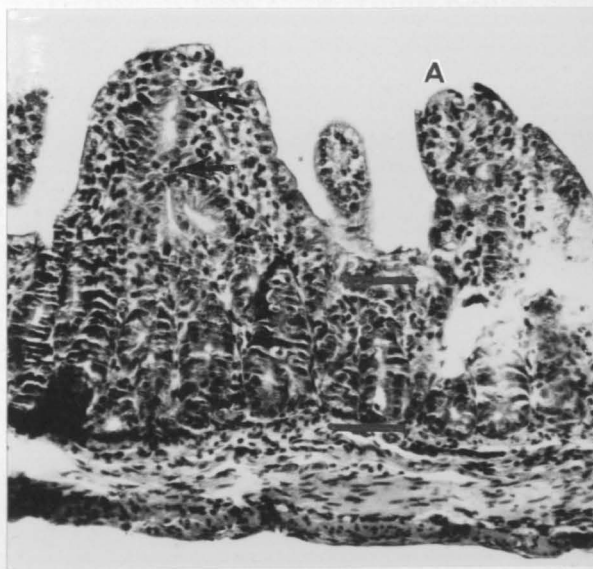
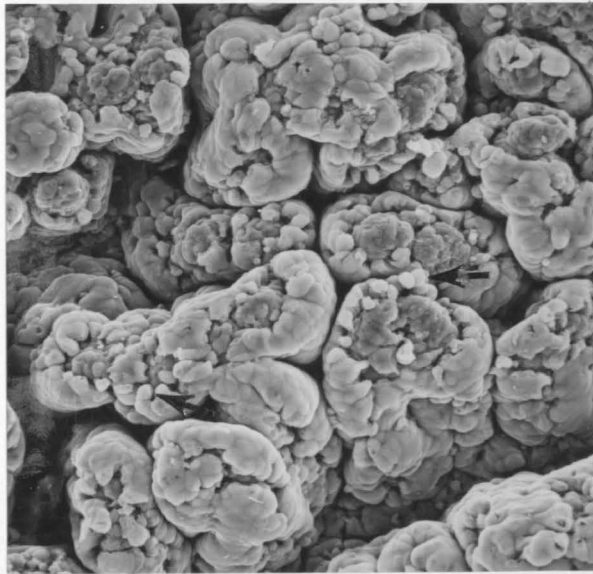


Figure 40. Scanning electron micrograph of the mid intestine 84 hours PI. Epithelial cells have regained their columnar form (C), and microvilli are intact (arrow). X 650.

Figure 41. Scanning electron micrograph of the upper ileum 84 hours PI. Villi are more individual but still severely shortened. Although lamina propria is exposed (L), epithelial cells are more columnar in nature (arrow). Compare to Fig. 42. X 200.

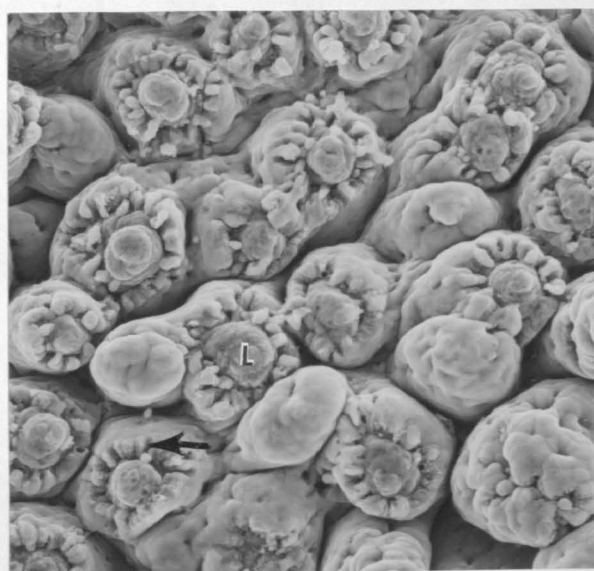
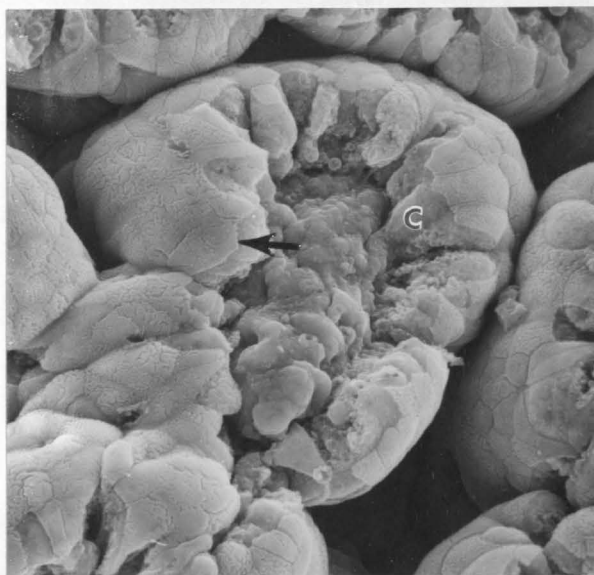


Figure 42. Scanning electron micrograph of the upper ileum control at 96 hours. Villi are irregularly shaped, epithelial cells are clearly defined, and some villi do not have a complete epithelial cell covering on the extrusion zone (arrow). X 120.

the surface.

The surface of the particles is very irregular and rough. The particles are of various sizes, ranging from about 10 to 100  $\mu\text{m}$ . The particles are of various shapes, ranging from spherical to elongated. The particles are of various colors, ranging from white to black. The particles are of various textures, ranging from smooth to rough. The particles are of various densities, ranging from light to heavy. The particles are of various compositions, ranging from pure to mixed. The particles are of various origins, ranging from natural to synthetic. The particles are of various uses, ranging from decorative to functional. The particles are of various properties, ranging from stable to unstable. The particles are of various characteristics, ranging from simple to complex. The particles are of various features, ranging from basic to advanced. The particles are of various attributes, ranging from common to rare. The particles are of various qualities, ranging from poor to good. The particles are of various quantities, ranging from small to large. The particles are of various amounts, ranging from little to much. The particles are of various degrees, ranging from low to high. The particles are of various levels, ranging from basic to advanced. The particles are of various stages, ranging from early to late. The particles are of various phases, ranging from initial to final. The particles are of various periods, ranging from short to long. The particles are of various times, ranging from quick to slow. The particles are of various durations, ranging from brief to extended. The particles are of various intervals, ranging from frequent to infrequent. The particles are of various frequencies, ranging from low to high. The particles are of various rates, ranging from slow to fast. The particles are of various speeds, ranging from slow to fast. The particles are of various velocities, ranging from slow to fast. The particles are of various accelerations, ranging from slow to fast. The particles are of various decelerations, ranging from slow to fast. The particles are of various directions, ranging from straight to curved. The particles are of various paths, ranging from simple to complex. The particles are of various trajectories, ranging from straight to curved. The particles are of various orbits, ranging from circular to elliptical. The particles are of various cycles, ranging from short to long. The particles are of various periods, ranging from short to long. The particles are of various times, ranging from quick to slow. The particles are of various durations, ranging from brief to extended. The particles are of various intervals, ranging from frequent to infrequent. The particles are of various frequencies, ranging from low to high. The particles are of various rates, ranging from slow to fast. The particles are of various speeds, ranging from slow to fast. The particles are of various velocities, ranging from slow to fast. The particles are of various accelerations, ranging from slow to fast. The particles are of various decelerations, ranging from slow to fast. The particles are of various directions, ranging from straight to curved. The particles are of various paths, ranging from simple to complex. The particles are of various trajectories, ranging from straight to curved. The particles are of various orbits, ranging from circular to elliptical. The particles are of various cycles, ranging from short to long.



### 96 Hours

Exposure of the lamina propria was reduced significantly in all sections. Lengthening of the villi was most apparent in the jejunum. Villi appeared to be separating and more individual below the fused tips, with occasional fusion points along the length of the villi (Fig. 43). Rounded epithelial cells on the sides of the regenerating villi still showed reduced microvilli numbers (Fig. 45). By LM, lengthening of villi was apparent with neighboring villi still fused at the top and sides (Fig. 44). In the mid intestine, the amount of exposed lamina propria area was less than that at 84 hours after inoculation. Epithelial cells on the tips of villi were no longer rounded (Fig. 46). In some areas of the mid intestine, exposure of the lamina propria was almost nonexistent although long creases remained on the top of villus clumps. The intestinal floor was no longer visible between individual or fused villi (Fig. 47). Light microscopy of the mid intestine showed villi to be lengthening, with the epithelial cell layer almost completely covering the villi (Fig. 48). At 96 hours, control mid intestinal villi were irregular in length with a pebbly appearance from slightly prominent epithelial cells (Fig. 49). Large amounts of mucus were present on the lower ileum villi and red blood cells could be seen on the surface of some villi (Fig. 50). Control lower ileum villi were quite misshapen and most villi did not have a complete epithelial cell layer over the extrusion zone, exposing either the basement membrane or the lamina propria (Fig. 51).

Figure 43. Scanning electron micrograph of the upper jejunum 96 hours PI. Villi are increasing in length and separation. of fused villi is more apparent. Villi tips are still fused (F), and fusion is visible between the sides of the villi (arrows). Rounded epithelial cells are present of the villus surface. Compare to Fig. 27. X 130.

Figure 44. Light micrograph of the lower jejunum 96 hours PI. An increase in separation and length of villi is apparent but fusion is still evident between villi and at the villi tips (arrows). Detachment of the epithelial cells (E) is probably an artifact. Compare to Fig. 28. X 110.

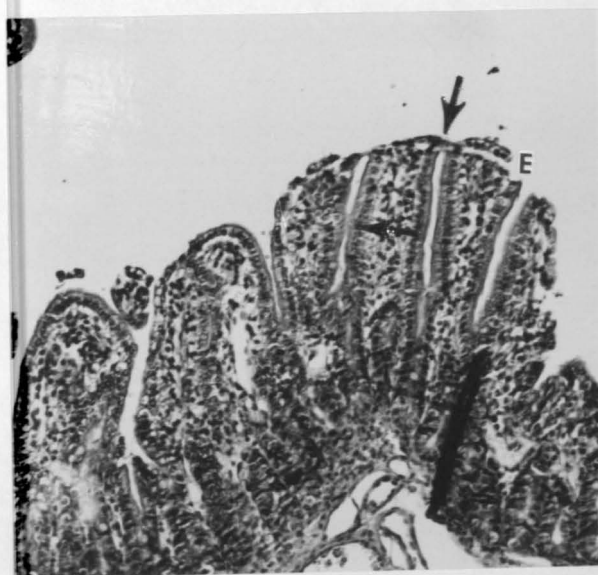
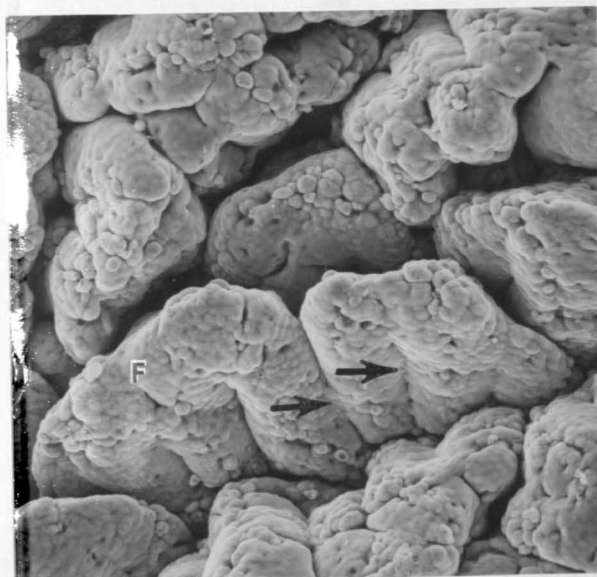




Figure 45. Scanning electron micrograph of two rounded epithelial cells on the side of a villus from the upper jejunum 96 hours PI. The protruding cells show a reduced number of microvilli. Compare to Fig. 34. X 1,800.

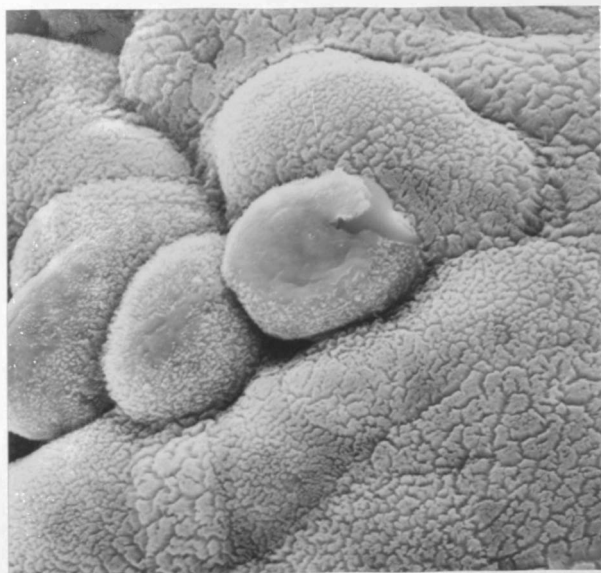


Figure 46. Scanning electron micrograph of the mid intestine 96 hours PI. Lamina propria (LP) exposure is lessening. Rounding of epithelial cells is not obvious as epithelial cells are columnar in shape (arrow). Compare to Fig. 49. X 300.

Figure 47. Scanning electron micrograph of the mid intestine 96 hours PI. Villi are more individual although fusion is still evident (F). Lamina propria exposure is not present. Long creases remain on the top of villus clusters (arrows). The intestinal floor is no longer visible. Compare to Fig. 49. X 130.

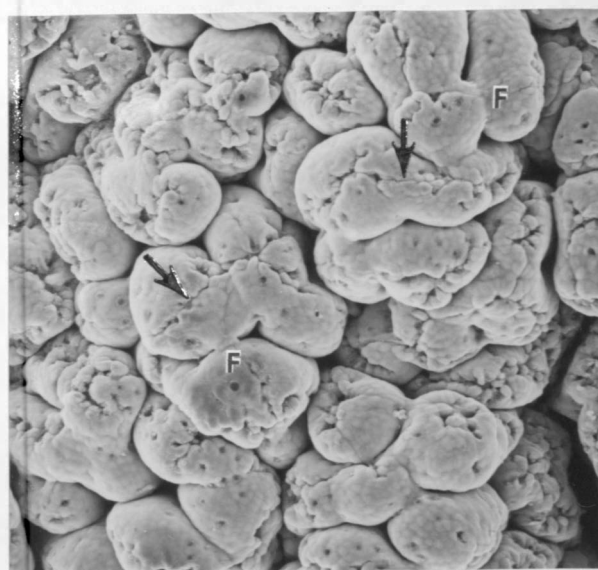
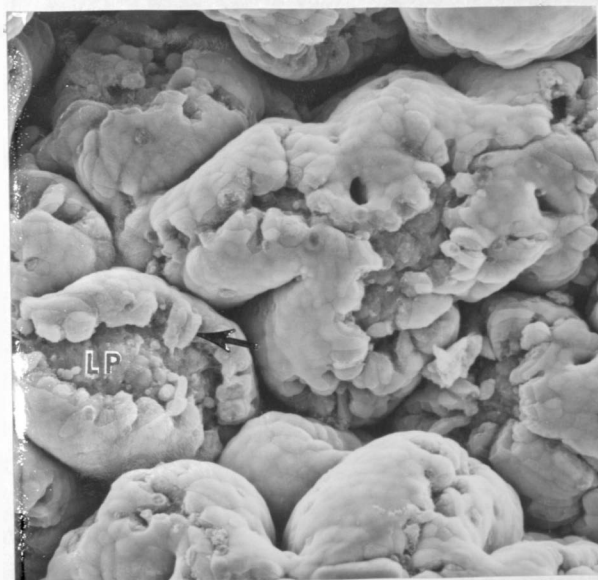


Figure 48. Light micrograph of the mid intestine 96 hours PI. Fusion is evident between villus tips (F) and along villus sides (arrows). The epithelial cell layer is complete except for a small opening (R). X 165.

Figure 49. Scanning electron micrograph of the control mid intestine at 96 hours. Villi are of varying lengths with slightly prominent epithelial cells resulting in a pebbly appearance. Exuded mucus is present on the villus sides (arrows). X 120.

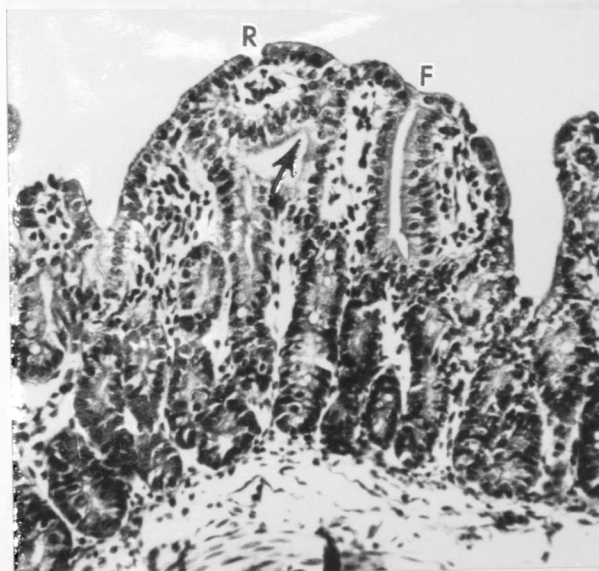
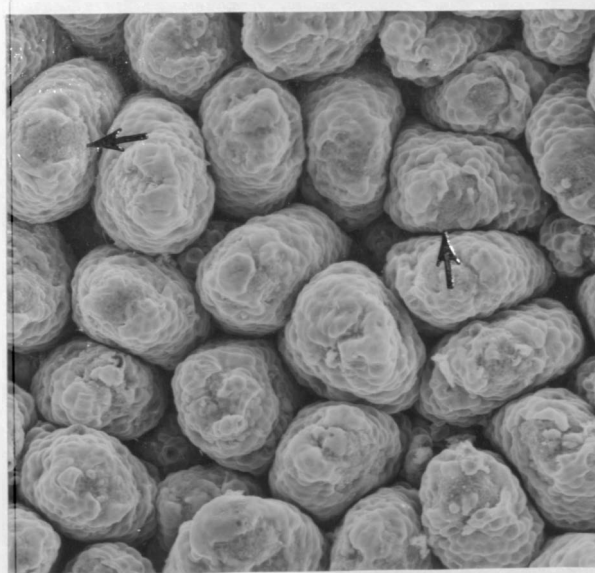
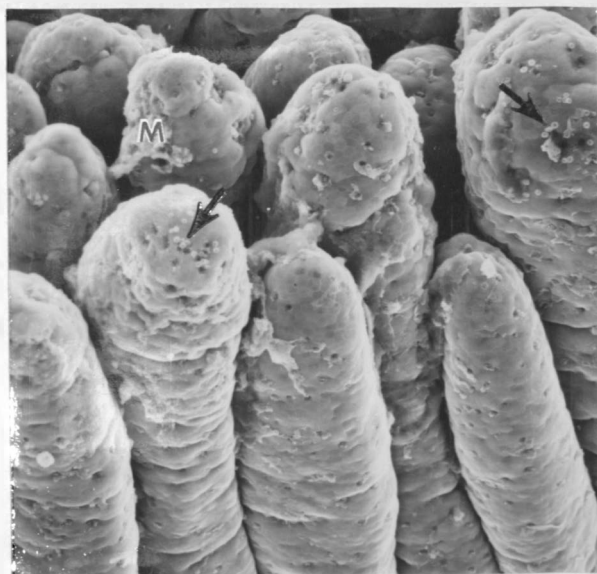


Figure 50. Scanning electron micrograph of the lower ileum 96 hours PI. Villi are long and broad with no indication of fusion or epithelial cell prominence. Large deposits of mucus (M) are apparent between villi and red blood cells can be seen on the villus tips (arrows). Compare to Fig. 51. X 150.

Figure 51. Scanning electron micrograph of the control lower ileum at 96 hours. Villus tips are irregularly shaped. Many villi do not have an intact epithelial cell layer resulting in exposure of the villus interior (arrows). X 130.





TRIAL 2

Examination of intestinal segments from this group of infected pigs revealed moderate villus atrophy, villus fusion and little villus shortening, which was not observed until 144 hours PI. Based on information obtained by examination of intestinal segments from the first set of gnotobiotic pigs, villus regeneration was expected to be significant at 144 hours PI. Because of the mild nature of the lesions observed, regenerative changes were not apparent and no data or micrographs will be presented.

### DISCUSSION

Using SEM and light microscopy (LM), villus shortening, exposure of the lamina propria, and fusion of villi in the intestine of pigs infected with rotavirus was noted. The most severe lesions were found in pigs necropsied 72 and 84 hours post inoculation (PI). These changes result in an intestine which would not function normally, leading to malabsorption and diarrhea. Villus shortening and damage to epithelial cells on villus tips causes reduction in the total mucosal surface area resulting in a decreased absorptive capacity. The loss of microvilli results in decreased beta-galactosidase and lactase enzymes, reduced surface area, and reduced digestive capacities (33,61).

Osmolarity and distribution of ions is also important in the development of diarrhea. When energy metabolism of the epithelial cells is disrupted, sodium, responsible for holding water in the extracellular fluid, may enter the cells releasing water in the extracellular fluid (56). When net secretion exceeds net absorption, diarrhea results (61).

When dealing with intestinal surfaces, SEM represents a faster easier, and more accurate way of obtaining information than LM. Because of the large area of tissue immediately visible by SEM and its three-dimensional aspect, certain morphologic features are visible that could otherwise be missed by serial sectioning. However, because the results of SEM are limited to surface information, other methods of examination (primarily light and transmission electron microscopy) should be applied to obtain internal cellular detail for a complete

and accurate representation of pathologic processes. Toner (83) discussed the importance of serial sectioning and LM. Although he refers to the binocular microscope, the principle also applies to the SEM:

"Although . . . surface examination (can) differentiate grossly abnormal from normal biopsies, . . . it can be no substitute for full serial sectioning of biopsies. Normal villi lying on their sides may give the impression of abnormality, while mild abnormalities detected by serial sectioning may not be apparent when only the tips of the villi are observed in the binocular microscope."

When examined by SEM, the first signs of infection, withdrawal of the villus tips, appears in the upper small intestine 12 hours PI (Fig. 1). This is in agreement with the fact that rotavirus has a predilection for the epithelial cells on the villus tips (61). Because villi in the infant animal divide and increase in number during growth of the intestine (9), the bifid or double tipped villi present at 12 hours PI (Fig. 1) are presumed to be normal.

The involvement of the lower ileum 12 hours and especially 24 hours PI is noteworthy (Figs. 5,9). Lesions in the lower ileum developed earlier and were more severe than lesions of other intestinal areas at these times. Examination by both SEM and LM revealed damage to the villi 24 hours PI (Figs. 13,15), although examination by transmission electron microscopy did not reveal any viral particles present in the lower ileum at this time (7). The ratio of infected cells to healthy cells was low, and this may account for the inability to demonstrate the presence of virus particles. Recovery of the lower ileum was rapid, and although the villi did not have the

regularly prominent epithelial cells of the control villi (Fig. 14), from 36 hours to 96 hours PI, the lower ileum appeared unaffected as viewed by SEM (Figs. 20,50). The rounded, prominent epithelial cells that have been observed in the ileum of gnotobiotic pigs by SEM are considered normal (63).

Examination by LM revealed an increased number of vacuoles in the villus epithelium of the lower intestine of the control pigs as compared to the upper intestine (Figs. 4,8). This is in agreement with the results of other work (19,59) which has shown more vacuoles present in ileal epithelium than in that of the duodenum or jejunum, and that the vacuoles persist from birth to two to four weeks. This also corresponds well with the increased prominence of epithelial cells in the ileum as observed by SEM. The increased prominence of these epithelial cells may result from vacuoles within the cell.

With the exception of the 12 hour PI pig, infected pig intestine, when viewed by LM, showed little, if any, vacuolation of villus epithelium (Figs. 23,39). On the other hand, Pearson and McNulty (67) observed vacuolation of villus epithelium in pigs at 24 and 29 hours PI and postulated that it resulted from the rotavirus infection. As in the infected pigs here, conventional (non-germfree) pigs lack vacuolation (60). This lack of vacuolation and the absence of prominent epithelial cells apparently results when certain substances are introduced into the newborn pig. An example of this could be when conventional pigs develop the normal intestinal flora, ingest colostrum or, in this case, when gnotobiotic pigs have been infected with rotavirus.

This maturation of the intestinal villi may help to explain the marked difference between the experimental lower ileum tissues and the control lower ileum tissues (Figs. 35,36). As the age of the control pigs increased, the number of ileal villi with incomplete epithelial cell covering and exposed lamina propria increased (Figs. 14,51). In the past, examination by LM has revealed exposed lamina propria of the villus tips in the normal ileum, although the pig's age at necropsy was not given (65). Because there is no colostrum or normal flora in the gnotobiotic pig's intestine, epithelial cells of the lower ileum may not be stimulated to move rapidly upward to cover the tips of the villi. In support of this idea, the turnover rate of the ileal epithelium in conventional mice was found to be significantly higher than that of germfree mice (1). The importance of the intestinal flora (in this case, rotaviruses) was further summarized: "The normal bacterial flora is seen to be one factor that plays a definitive role in the establishment of the 'normal' equilibrium of this complex system" (1). Therefore, the difference in appearance of the infected lower ileum as compared to the appearance of the control lower ileum may not be a lesion. Instead, the lack of rounded ileal epithelial cells may be a manifestation of the normal morphogenesis of the villi as they mature (i.e. contacts microbial flora) and the protective function of the epithelial cells comes into being.

Another early indication of infection, along with withdrawal of the villus tips, is the rounding and sloughing of epithelial cells in the lower jejunum 24 hours PI (Figs. 9,10). It is possible that their

presence on the villus tip is exaggerated because the villus contracts in response to the infection. The long ridge of tissue present in the mid intestine of the 24 hour PI pig (Fig. 12) has not been reported in studies on normal or infected intestinal mucosa. Its origin and purpose is unknown. Ridged epithelium is known to occur although this is in animals other than pigs (67).

When examined by SEM, only the upper intestine appeared affected in pigs infected 36 hours, and the duodenum was the most severely affected (Fig. 16). However, when examined by LM, all areas of the intestine had shortened villi. Examination by SEM revealed the progression of lesions had subsided in pigs infected 48 and 60 hours although by LM examination villi remained shortened. The apparent decrease in epithelial cell rounding and lamina propria exposure at these times may be attributed to any or all of three things. First, this may be caused by the virus replication cycle. Initial infection results in degeneration and rounding of the epithelial cells followed by a reinfection of new cells. During virus replication, these changes subside. After the release of a majority of mature virus particles and a reinfection of new cells (possibly around 72 hours PI as direct examination of virus laden fecal material suggests) (7), the changes in villus structure and appearance are more severe. Second, variation in the sequence of infection may be related to individual variation in each pig's response to the infection. Third, the number of infectious particles may have varied from one inoculum to another.

Exposure of the lamina propria and fusion of villi are the ultimate lesions of rotavirus infection in gnotobiotic pigs. When rounded epithelial cells are sloughed off the villi faster than they are replaced, exposure of the lamina propria results. Epithelial cells on the villus surface and around the exposed lamina propria remain rounded during the active infection (52,53,54), but revert to columnar form as recovery and regeneration progresses. Villus fusion was observed in some intestinal segments at 12 hours PI without appreciable lamina propria exposure. This may result from an adherence phenomenon (67) in which adjacent villi show a cellular continuity at certain points.

Villus regeneration characterized by increase in length and individualization could be noted 84 hours PI by both SEM and LM. The regeneration continued 96 hours after infection (Figs. 39,43,44). Additionally, as seen by LM, crypt hyperplasia (explained later) indicated ongoing villus regeneration (Fig. 39). By this time, epithelial cells have regained their columnar shape and appear to be moving up from the crypts unhindered (Figs. 40,46). The long creases on the tips of the villus clusters are caused by the meeting of the epithelial cell layers as they cover and enclose the exposed lamina propria (Fig. 47). Red blood cells present on the villi of the lower jejunum at 96 hours PI (Fig. 50) probably originated from damaged lamina propria in intestinal areas in the upper intestine.

Crypt hyperplasia (lengthening and thickening of the crypts of Lieberkuhn) is used as an indication of villus regeneration, and often

expressed as a ratio of the villus length to the crypt length (V:C). In uninfected pigs, the V:C may be as high as 13.0 while in the later stages of infection before regeneration, it may be reduced to 0.5 (67). The hyperplastic crypts show an increase in mitotic activity and speed up production of immature epithelial cells to migrate upward, mature, and replace those cells damaged by infection (61).

Although the second set of gnotobiotic pigs inoculated with fecal material from the first set of gnotobiotic pigs was examined over a period of 144 hours, the villi did not regenerate after infection as expected. Instead, the lesions were less severe and maximum villus atrophy was not reached until 144 hours PI when regeneration was expected. This may have been caused by a decrease in the virulence of the rotavirus after its passage through gnotobiotic pigs. On the other hand, the time after onset of diarrhea that the virus inoculum is collected may have influenced its virulence (discussed later). This reduction in virulence is in agreement with that in other reports (47). However, the calf rotavirus, after passage through gnotobiotic calves, shows an increase in virulence and a corresponding decrease in the time before maximum villus atrophy is reached (54).

Microvilli were easily discernable by SEM (Fig. 34) and the mucus or "fuzzy coat" encountered by other investigators (5,24,45,57,62) caused little obstruction of detail. Use of the  $\text{OsO}_4$ -TCH technique instead of the evaporative metal technique may have prevented obscured microvilli detail and allowed accurate determinations of microvilli width. Although it is known to occur in TGE infections (78), reduction in microvilli numbers visualized by SEM has not been reported in rotavirus



infections. Reduction in microvilli numbers is normal as cells degenerate at the extrusion zone (82), but on abnormally rounded epithelial cells on the tips and sides of villi it should be considered a lesion.

The lesions observed in this study are similiar, but not identical to those that occur in pigs with enteritis caused by TGE virus, and those that occur in calves with calf rotavirus or infantile diarrhea virus. Incubation time of pig rotavirus infection appears to be longer than that of the other types of enteric viruses. Maximum villus atrophy occurs 60 to 84 hours PI, whereas in TGE virus infections, maximum villus atrophy, including severe shortening or near complete destruction of the villi, occurs more rapidly and appears as early as 24 to 48 hours after exposure (31,37,65,88). The exact time sequence and degree of villus atrophy caused by the calf rotavirus in calves has not yet been ascertained. However, in calves infected with virus obtained from filtered diarrhetic material, villi in the caudal part of the small intestine 47 hours PI were shortened and covered with epithelial cells of irregular size and shape. In addition, when the virus used as inoculum had undergone passage through gnotobiotic calves, the time lapse from inoculation to onset of diarrhea was reduced to 14 hours. In this instance, many villi in the caudal part of the small intestine were shortened and denuded at their tips (54). Gnotobiotic calves infected with the infantile gastroenteritis virus had denuded villi 28 hours PI (55).

The presence of many fused villi from the lower jejunum to the upper ileum 72, 84, and 96 hours PI has not been reported in other

rotavirus studies. Pearson and McNulty (67) reported that fused villi were common from 48 hours to 168 hours PI although the locations and extent of fusion were not given. Fusion of the villi in TGE infected swine has been reported (85,88) but this is not the primary lesion. Complete villus destruction takes place so rapidly that epithelial cell migration up from the crypts does not occur fast enough to enclose fused villi. Although denuded villi and exposure of the lamina propria have not been reported in colibacillosis studies (18,41), its importance as a lesion has recently been discussed (63).

Major differences in results exists between this study and the results of other studies on rotaviral and TGE infections. The involvement of the duodenum 36 hours PI resulting in villus shortening and fusion is a significant difference (Fig. 16). In TGE, the villi in the duodenum have been found to remain normal (22,37,69,79,87), or in some cases, slightly shortened (85,88). It has been suggested that bile excreted into the duodenum may inactivate the ether-sensitive TGE virus and protect the duodenum from infection (36). As the bile moves through the intestinal tract, it is diluted with other fluids, reducing its antiviral properties and allowing viral damage to the lower intestine. Since rotaviruses are ether resistant (89), the effects of bile on the virus may be reduced. However, Pearson and McNulty (67) were unable to observe any histologic changes in the duodenum of pigs infected with the pig rotavirus until 96 hours PI when the primary lesion was villus shortening. Duodenal infections may occur with the calf rotavirus. Studies have either not included the duodenum per se,

or measurements given for the location of the "upper" intestinal segment have been too far from the pyloric valve to include the duodenum (50,54).

Hooper (38) has shown that in mice the epithelium in the duodenum is replaced more rapidly than that in either the jejunum or ileum. If this is true in pigs, the rapid epithelial replacement time may help to explain the lack of denuded villi in the duodenum 36 hours PI and the apparent uninvolved state at subsequent hours. Moon (58) however, found replacement times of the duodenal epithelium in suckling pigs to be equal to the replacement times of the epithelium of the remainder of the intestine. Whether a difference exists in gnotobiotic pigs or not is unknown.

Theil et al. (81), in studies on rotaviral infections in pigs, used a rotavirus inoculum derived after seven passages in gnotobiotic pigs. At PI times comparable to those in this study, they were unable to show by immunofluorescence viral antigen in 7 of 15 duodenal intestinal segments taken from the intestine of infected pigs in three separate experiments. In this study, fluorescence was found in all duodenal segments even at 12 hours PI (7).

Examination of fecal material from pigs used in this study showed that early in the infection, although the pigs were suffering from viral induced diarrhea, 2/3 of the virus particles excreted were incomplete. It was not until 72 hours PI that most of the viral particles were complete (7). If Theil et al. (81) collected virus samples early in the development of diarrhea for passage to subsequent

gnotobiotic pigs, it is possible that they were selecting for incomplete particles, with a minority of complete particles responsible for the diarrhea. Because the duodenum is the least affected in pig rotavirus infections (excepting the lower ileum), lowering the number of infectious particles may lower the incidence of infection in the duodenum. Likewise, in this study, when an inoculum was prepared for the second set of gnotobiotic pigs, fecal samples were collected from the early stages of diarrhea in the first set of gnotobiotic pigs. The resulting infection had a decrease in the severity of villus atrophy and a doubling of the time before atrophy occurred.

In gnotobiotic calves infected with the NCD virus, Mebus (50) found fluorescence on the tips of villi in the upper small intestine, or, more commonly, no fluorescence at all. An increasing amount of fluorescence was noted from the middle to the lower intestine. Their explanation for the lack of fluorescence in the upper small intestine was related to the time lag from onset of diarrhea to necropsy. Initial infection begins in the upper small intestine and progresses distally. Since the crypt cells are not affected in rotaviral infections (61), epithelial cells are continually moving up the villi to replace infected cells released at the extrusion zone or on the villus sides. These new cells are apparently resistant to reinfection (50). As diarrhea symptoms lag behind the virus infection of cells, in calves killed 0.5 to 1.0 hours after the onset of diarrhea, the villi in the upper small intestine have fluorescent cells only on the tip, with fluorescing cells covering the outer 1/3 to 3/4 of the villi in

the remainder of the intestine. On the other hand, in calves killed 4.5 hours following the onset of diarrhea, no immunofluorescence was observed in the small intestinal epithelium (50). The lack of fluorescence could be explained by assuming either a very rapid replacement time for intestinal epithelium in the calf, or an inoculum reduced in virulence.

The suggested time lag between rotaviral infection of epithelial cells and the onset of diarrhea in calves (50) was not evident in infected pigs in this study. Virus particles were observed in villus epithelium 12 hours PI when diarrhea began (7).

The results of this study have also demonstrated a striking difference in the response of the upper and lower ileum of the pig to rotavirus infection. The epithelium of the lower ileum of gnotobiotic pigs is the most susceptible to initial infection by the pig rotavirus at 24 hours PI (Fig. 13). Although demonstration of viral antigen by fluorescent antibody tests were not consistent with this (7), villi in each intestinal section were not equally affected by the rotavirus which could account for variability in the results. This patchy involvement of the intestinal mucosa to rotaviral infection was also observed by Pearson and McNulty (67).

Additionally, epithelium of the lower ileum has the capacity for the most rapid recovery. Table 2 and Figures 31 and 35 show that while the upper ileum was severely affected, the lower ileum was uninvolved. Although Pearson and McNulty (67) found a decrease in the ileal V:C ratio at 24 hours PI, corresponding to the shortened villi demonstrated

here (Fig. 13), they also found villus height and the V:C ratio to be depressed through 168 hours PI which was not evident in this study. In calves infected with the calf rotavirus, the appearance of the lower small intestine was similiar to that of control tissues of the lower small intestine with one exception where occasional denuded villi were noted (50).

Because of the demonstrated difference in appearance and response of the villi in the upper and lower ileum to rotaviral infection, it is difficult to relate these results to results of other rotavirus studies where the location of the lower intestinal segment is vague. In subsequent studies of rotaviral infections, designations such as distal, terminal, caudal, and lower intestine should be avoided and exacting comparisons made with control segments from the same location. It is not known whether the difference in the upper and lower ileum response is related to the animal species studied, which species of rotavirus is involved, or both.

It should be noted that this study involved the pathogenesis of rotaviral infection in gnotobiotic pigs which may or may not accurately correspond to the pathogenesis in conventional pigs. The role of bacteria in the development or enhancement of rotaviral infections is under question and study (10,26,33,42). Also, only one pig was used at each time interval and individual variation among pigs may cause some discrepancies in the observed results. Clearly, more work needs to be done on both gnotobiotic and conventional pigs to accurately determine the pathogenesis of rotaviruses.

### SUMMARY

Scanning electron microscopy (SEM) has proven to be a valuable tool in the study of intestinal responses to rotaviral infection. The OsO<sub>4</sub>-thiocarbohydrazide technique of specimen preparation allows visualization of fine details as well as an improvement in image formation produced by a more even coating and more efficient secondary electron emission than the evaporated metal technique.

Scanning electron and light microscopy were used to examine intestinal segments of gnotobiotic pigs infected with rotavirus. Lesions observed were rounding of epithelial cells at the extrusion zone and along the sides of villi, shortening and fusion of villi, and exposure of the lamina propria. The first evidence of infection, withdrawal of the villus tip, was observed 12 hours post inoculation (PI). At 24 hours PI, rounding of epithelial cells was observed in all intestinal sections except the duodenum. Extensive villus contraction and exposure of the lamina propria, but no fusion, was observed in the lower ileum at 24 hours PI. Villus shortening, fusion and rounded epithelial cells were observed by SEM in the duodenum at 36 hours PI. From 36 hours to 96 hours PI, light microscopy showed villi to be shortened in the lower ileum although villi appeared normal by SEM except for the lack of prominent, bulging epithelial cells present on the control lower ileum villi. Lesions subsided until 72 hours and 84 hours PI when maximum villus atrophy was noted. Villi in all intestinal segments except the duodenum and lower ileum were severely stunted and fused into irregular clusters with exposure

of the lamina propria. Villus regeneration was beginning at 84 hours PI and continuing at 96 hours PI as evidenced by replacement of the epithelial cells over the exposed lamina propria and lengthening of the villi. Because of the duration of the experiment, the extent of villus regeneration could not be determined.

3. Lippman, H., A. B. Johnson, and F. S. Jones. 1973. "Regulation of Epithelial Proliferation in the Small Intestine of the Rat." *Am. J. Pathol.* 81: 111-121.
4. Lippman, H., A. B. Johnson, L. H. Jones, M. J. Jones, and F. S. Jones. 1975. "Regulation of Epithelial Proliferation in the Small Intestine of the Rat." *Am. J. Pathol.* 83: 111-121.
5. Lippman, H., A. B. Johnson, and F. S. Jones. 1975. "Regulation of Epithelial Proliferation in the Small Intestine of the Rat." *Am. J. Pathol.* 83: 111-121.
6. Lippman, H., A. B. Johnson, and F. S. Jones. 1975. "Regulation of Epithelial Proliferation in the Small Intestine of the Rat." *Am. J. Pathol.* 83: 111-121.
7. Lippman, H., A. B. Johnson, and F. S. Jones. 1975. "Regulation of Epithelial Proliferation in the Small Intestine of the Rat." *Am. J. Pathol.* 83: 111-121.
8. Lippman, H., A. B. Johnson, and F. S. Jones. 1975. "Regulation of Epithelial Proliferation in the Small Intestine of the Rat." *Am. J. Pathol.* 83: 111-121.
9. Lippman, H., A. B. Johnson, and F. S. Jones. 1975. "Regulation of Epithelial Proliferation in the Small Intestine of the Rat." *Am. J. Pathol.* 83: 111-121.
10. Lippman, H., A. B. Johnson, and F. S. Jones. 1975. "Regulation of Epithelial Proliferation in the Small Intestine of the Rat." *Am. J. Pathol.* 83: 111-121.
11. Lippman, H., A. B. Johnson, and F. S. Jones. 1975. "Regulation of Epithelial Proliferation in the Small Intestine of the Rat." *Am. J. Pathol.* 83: 111-121.
12. Lippman, H., A. B. Johnson, and F. S. Jones. 1975. "Regulation of Epithelial Proliferation in the Small Intestine of the Rat." *Am. J. Pathol.* 83: 111-121.



LITERATURE CITED

1. Abrams, G. D., H. Bauer, and H. Sprinz. 1963. Influence of the Normal Flora on Mucosal Morphology and Cellular Renewal in the Ileum. *Lab. Invest.* 12:355-364.
2. Anderson, T. F. 1956. *Electron Microscopy of Microorganisms. Physical Techniques in Biological Research. First Edition.* Academic Press. New York, New York. 3:177-240.
3. Asquith, P., A. G. Johnson, and W. T. Cooke. 1970. Scanning Electron Microscopy of Normal and Celiac Jejunal Mucosa. *Am. J. Dig. Dis.* 15:511-521.
4. Babiuk, L. A., K. Mohammed, L. Spence, M. Fauvel, and R. Petro. 1977. Rotavirus Isolation and Cultivation in the Presence of Trypsin. *J. Clin. Microbiol.* 6:610-617.
5. Balcerzak, S. P., W. C. Lane, and J. W. Bullard. 1970. Surface Structure of Intestinal Epithelium. *Gastroenterology.* 58:49-55.
6. Bartlett, A. A. and H. P. Borstyn. 1975. A Review of the Physics of Critical Point Drying. *Proc. 8th Ann. SEM Symposium ITT Res. Institute. Chicago, Ill.* 8:305-316.
7. Bergland, M., J. P. McAdaragh, M. Johnshoy, I. J. Stotz, R. C. Myer, and R. Hammer. 1978. Pathogenesis of Rotaviral Enteritis in Gnotobiotic Pigs: A Microscopic Study. To Be Published. *J. Am. Vet. Med. Assoc.*
8. Bishop, R. F., G. P. Davidson, I. H. Holmes, and R. J. Ruck. 1973. Virus Particles in the Epithelial Cells of Duodenal Mucosa from Children with Acute Nonbacterial Gastroenteritis. *Lancet.* 2:1281-1283.
9. Bloom, W. and D. W. Fawcett. 1968. *A Textbook of Histology. Ninth Edition.* W. B. Saunders Company. Philadelphia, Penn. pp. 560-581.
10. Bohl, E. H., E. M. Kohler, L. J. Saif, R. F. Cross, A. G. Agnes, and K. W. Theil. 1978. Rotavirus as a Cause of Diarrhea in Pigs. *J. Am. Vet. Med. Assoc.* 172:458-463.
11. Borden, E. C., R. E. Shope, and F. A. Murphy. 1971. Physiochemical and Morphological Relationships of Some Arthropod-Borne Viruses to Bluetongue-A New Taxonomic Group. *Physiochemical and Serological Studies. J. Gen. Virol.* 13:261-271.
12. Boyde, A. 1972. Biological Specimen Preparation for Scanning Electron Microscopy-A Review. *Proc. 5th Ann. SEM Symposium ITT Res. Institute. Chicago, Ill.* 5:257-264.

13. Boyde, A. and P. Vesely. 1972. Comparison of Fixation and Drying Procedures for Scanning Electron Microscopy. Proc. 5th Ann. SEM Symposium ITT Res. Institute. Chicago, Ill. 5:265-272.
14. Bridger, J. C., G. N. Woode, J. M. Jones, T. H. Flewett, A. S. Bryden, and H. Davies. 1975. Transmission of Human Rotavirus to Gnotobiotic Piglets. J. Med. Microbiol. 8:565-569.
15. Brown, A. L. 1962. Microvilli of the Human Jejunal Epithelial Cell. J. Cell. Biol. 12:623-627.
16. Bryden, A. S., M. F. Thouless, and T. H. Flewett. 1976. Rotavirus in Rabbits. (Letter). Vet. Rec. 99:323.
17. Cheever, F. S. and J. H. Mueller. 1947. Epidemic Diarrheal Disease of Suckling Mice. 1. Manifestations, Epidemiology, and Attempts to Transmit the Disease. J. Exp. Med. 85:405-416.
18. Christie, B. R. and G. L. Waxler. 1973. Experimental Colibacillosis in Gnotobiotic Baby Pigs. II. Pathology. Can. J. Comp. Med. 37:271-280.
19. Clarke, R. M. and R. N. Hardy. 1971. Histological Changes in the Small Intestine of the Young Pig and Their Relation to Macromolecular Uptake. J. Anat. (London). 108:63-77.
20. Cocco, A. E., M. M. Dohrmann, and T. R. Hendrix. 1966. Reconstruction of Normal Jejunal Biopsies: Three-Dimensional Histology. Gastroenterology. 51:24-31.
21. Cohen, A. L. 1977. A Critical Look at Critical Point Drying-Theory, Practice, and Artifacts. Proc. 10th Ann. SEM Symposium ITT Res. Institute. Chicago, Ill. 10:525-536.
22. Cross, R. F. and E. H. Bohl. 1969. Some Criteria for the Field Diagnosis of Porcine Transmissible Gastroenteritis. J. Am. Vet. Med. Assoc. 154:266-272.
23. Davidson, G. P., R. F. Bishop, R. R. W. Townley, I. H. Holmes, and B. F. Ruck. 1975. Importance of a New Virus in Acute Sporadic Enteritis in Children. Lancet. 1:242-246.
24. Demling, L., V. Becker, and M. Classen. 1969. Examinations of the Mucosa of the Small Intestine with the Scanning Electron Microscope. Digestion. 2:51-60.
25. DeNee, P. B. and E. R. Walker. 1975. Specimen Coating Techniques for the SEM-A Comparative Study. Proc. 8th Ann. Symposium ITT Res. Institute. Chicago, Ill. 8:225-232.

26. Escheverria, P., N. R. Blacklow, and D. H. Smith. 1975. Role of Heat-Labile Toxigenic Escherichia coli and Reovirus-Like Agent in Diarrhoea in Boston Children. *Lancet*. 2:1113-1116.
27. Echlin, P. 1975. Sputter Coating Techniques for Scanning Electron Microscopy. Proc. 8th Ann. Symposium ITT Res. Institute. Chicago, Ill. 8:217-224.
28. Espejo, R. T., E. Calderon, and N. Gonzalez. 1977. Distinct Reovirus-Like Agents Associated with Acute Infantile Gastroenteritis. *J. Clin. Microbiol.* 6:502-506.
29. Flewett, T. H., A. S. Bryden, H. Davies, G. N. Woode, J. Bridger, and J. M. Derrick. 1974. Relationship Between Viruses from Acute Gastroenteritis of Children and Newborn Calves. *Lancet*. 2:61-63.
30. Flewett, T. H., A. S. Bryden, and H. Davies. 1975. Virus Diarrhea in Foals and Other Animals. (Letter). *Vet. Rec.* 96:477.
31. Haelterman, E. O. 1972. On the Pathogenesis of Transmissible Gastroenteritis of Swine. *J. Am. Vet. Med. Assoc.* 160:534-546.
32. Hall, G. A., J. C. Bridger, R. L. Chandler, and G. N. Woode. 1976. Gnotobiotic Piglets Experimentally Infected with Neonatal Calf Diarrhoea Reovirus-Like Agent (Rotavirus). *J. Vet. Pathol.* 13:197-210.
33. Halpin, C. G. and I. W. Caple. 1976. Changes in Intestinal Structure and Function in Neonatal Calves Infected with Reovirus-Like Agent and Escherichia coli. *Aust. Vet. J.* 52:438-441.
34. Hayes, T. L. and R. F. W. Pease. 1968. The Scanning Electron Microscope: Principles and Applications in Biology and Medicine. Advances in Biological and Medical Physics. Ed. Lawrence, J. H. and J. W. Gofman. Academic Press. New York, New York. pp. 85-137.
35. Holmes, I. H., B. J. Ruck, R. F. Bishop, and G. P. Davidson. 1975. Infantile Enteritis Viruses: Morphogenesis and Morphology. *J. Virol.* 16:937-943.
36. Hooper, B. E. 1965. Transmissible Gastroenteritis of Swine: Studies on the Pathogenesis. Ph.D. Thesis. Purdue University.
37. Hooper, B. E. and E. O. Haelterman. 1969. Lesions of the Gastrointestinal Tract of Pigs Infected with Transmissible Gastroenteritis. *Can. J. Comp. Med.* 33:29-36.

38. Hooper, C. E. S. 1962. Methods for the Investigation of Cellular Renewal in the Intestinal Epithelium. *Meth. Med. Res.* 9:326-342.
39. Ito, S. 1965. The Enteric Surface Coat on Cat Intestinal Microvilli. *J. Cell. Biol.* 27:475-491.
40. Kelley, R. O., R. A. F. Dekker, and J. G. Bluemink. 1973. Ligand-Mediated Osmium Binding: Its Application in Coating Biological Specimens for Scanning Electron Microscopy. *J. Ultrastructure Research.* 45:254-258.
41. Kenworthy, R. 1970. Effects of *Escherichia coli* on Germ-Free and Gnotobiotic Pigs. I. Light and Electron Microscopy of the Small Intestine. *J. Comp. Pathol.* 80:53-63.
42. Leece, J. G., M. W. King, and R. Mock. 1976. Reovirus-Like Agent Associated with Fatal Diarrhea in Neonatal Pigs. *Infect. and Immun.* 14:816-825.
43. McNulty, M. S., G. M. Allan, G. R. Pearson, J. B. McFerran, W. B. Curran, and R. M. McCracken. 1976. Reovirus-Like Agent (Rotavirus) from Lambs. *Infect. and Immun.* 14:1332-1338.
44. Malick, L. E. and R. B. Wilson. 1975. Modified Thiocarbohydrazide Procedure for Scanning Electron Microscopy: Routine Use for Normal, Pathological, or Experimental Tissues. *Stain Tech.* 50:256-269.
45. Marsh, M. N. and J. A. Swift. 1969. A Study of the Small Intestinal Mucosa Using the Scanning Electron Microscope. *Gut.* 10:940-949.
46. Maser, M. D. and J. J. Trimble. 1977. Rapid Chemical Dehydration of Biological Samples for Scanning Electron Microscopy Using 2,2-Dimethoxypropane. *J. Histochem. Cytochem.* 25:247-251.
47. Mebus, C. A. Personal Communication.
48. Mebus, C. A., N. R. Underdahl, M. B. Rhodes, and M. J. Twiehaus. 1969. Calf Diarrhea (Scours): Reproduced with a Virus from a Field Outbreak. *Univ. Neb. Res. Bull.* 233:1-16.
49. Mebus, C. A., M. Kono, N. R. Underdahl, and M. J. Twiehaus. 1971. Cell Culture Propagation of Neonatal Calf Diarrhea (Scours) Virus. *Can. Vet. J.* 12:69-72.
- ✓ 50. Mebus, C. A., E. L. Stair, N. R. Underdahl, and M. J. Twiehaus. 1971. Pathology of Neonatal Calf Diarrhea Induced by a Reo-Like Virus. *Vet. Pathol.* 8:490-505.

51. Mebus, C. A., L. E. Newman, and E. L. Stair. 1975. Scanning Electron, Light, and Transmission Electron Microscopy of Intestine of Gnotobiotic Calf. *Am. J. Vet. Res.* 36:985-993.
52. Mebus, C. A. 1976. Calf Diarrhea Induced by Coronavirus and a Reovirus-Like Agent. *Mod. Vet. Pract.* 56:693-698.
53. Mebus, C. A., R. G. Wyatt, R. L. Sharpee, M. M. Sereno, A. R. Kalica, A. Z. Zapikian, and M. J. Twiehaus. 1976. Diarrhea in Gnotobiotic Calves Caused by the Reovirus-Like Agent of Human Infantile Gastroenteritis. *Infect. and Immun.* 14:471-474.
54. Mebus, C. A. and L. E. Newman. 1977. Scanning Electron, Light, and Immunofluorescent Microscopy of Intestine of Gnotobiotic Calf Infected with Reovirus-Like Agent. *Am. J. Vet. Res.* 38:553-558.
55. Mebus, C. A., R. G. Wyatt, and A. Z. Zapikian. 1977. Intestinal Lesions Induced in Gnotobiotic Calves by the Virus of Human Infantile Gastroenteritis. *Vet. Pathol.* 14:273-282.
56. Michell, A. R. 1974. Body Fluids and Diarrhoea: Dynamics of Dysfunction. *Vet. Rec.* 94:311-315.
57. Millington, P. F., D. R. Critchley, P. W. A. Tovell, and R. Pearson. 1969. Scanning Electron Microscopy of Intestinal Microvilli. *J. Micros.* 89:339-344.
58. Moon, H. W. 1971. Epithelial Cell Migration in the Alimentary Mucosa of the Suckling Pig. *Proc. Soc. Exp. Biol. Med.* 137:151-154.
59. Moon, H. W. 1972. Vacuolated Villous Epithelium of the Small Intestine of Young Pigs. *Vet. Pathol.* 9:3-21.
60. Moon, H. W., E. M. Kohler, and S. C. Whipp. 1973. Vacuolization: A Function of Cell Age in Porcine Absorptive Cells. *Lab. Invest.* 28:23-28.
61. Moon, H. W. 1978. Mechanisms in the Pathogenesis of Diarrhea: A Review. *J. Am. Vet. Med. Assoc.* 172:443-448.
62. Mouwen, J. M. V. M. 1971. White Scours in Piglets. II. Scanning Electron Microscopy of the Mucosa of the Small Intestine. *Vet. Pathol.* 8:401-413.
63. Newman, L. E., A. L. Trapp, and G. L. Waxler. 1977. Lesions of Experimentally Induced Colibacillosis in Neonatal Gnotobiotic Pigs: A Scanning Electron Microscopic Study. *Am. J. Vet. Res.* 38:297-305.

64. Oatley, C. W., W. C. Nixon, and R. F. W. Pease. 1965. Scanning Electron Microscopy. Advances in Electronics and Electron Physics. Ed. Marton, L. Academic Press, New York, New York. pp. 181-247.
65. Olson, D. P., G. L. Waxler, and A. W. Roberts. 1973. Small Intestinal Lesions of Transmissible Gastroenteritis in Gnotobiotic Pigs: A Scanning Electron Microscopic Study. Am. J. Vet. Res. 34:1239-1245.
66. Padykula, H. A. 1962. Recent Functional Interpretations of Intestinal Morphology. Gastroenterology. 21:873-879.
67. Pearson, G. R. and M. S. McNulty. 1977. Pathological Changes in the Small Intestine of Neonatal Pigs Infected with a Pig Reovirus-Like Agent (Rotavirus). J. Comp. Pathol. 87:363-375.
68. Pease, R. F. W. 1971. Fundamentals of Scanning Electron Microscopy. Proc. 4th Ann. SEM Symposium ITT Res. Institute. Chicago, Ill. 4:9-16.
69. Pensaert, M., E. O. Haelterman, and T. Burnstein. 1970. Transmissible Gastroenteritis of Swine: Virus-Intestinal Cell Interactions. 1. Immunofluorescence, Histopathology, and Virus Production in the Small Intestine through the Course of Infection. Arch. ges Virusforsch. 31:321-334.
70. Petric, M., P. J. Middleton, C. Grant, J. S. Tam, and C. M. Hewitt. 1978. Lapine Rotavirus: Preliminary Studies on Epizootology and Transmission. Can. J. Comp. Med. 42:143-147.
71. Pfeiffer, C. J. 1968. Intestinal Villous Morphology. Post Grad. Medicine. 43:215-221.
72. Reed, D. R., C. A. Daley, and H. J. Shave. 1976. Reovirus-Like Agent Associated with Neonatal Diarrhea in Pronghorn Antelope. J. Wild. Dis. 12:488-491.
73. Rubenstein, D., R. G. Milne, R. Buckland, and D. A. J. Tyrrell. 1971. The Growth of the Virus of the Epidemic Diarrhoea of Infant Mice (EDIM) in Organ Cultures of Intestinal Epithelium. Br. J. Exp. Pathol. 53:442-445.
74. Sessions, J. T., S. R. Viegas de Angrade, and E. Kokas. 1968. Intestinal Villi: Form and Motility in Relation to Function. Progress in Gastroenterology. Volume One. Ed. Glass, G. B. J. Grune and Stratton. New York, New York. pp. 248-260.

75. Sheehy, T. W. and M. F. Floch. 1964. The Small Intestine: Its Function and Diseases. Harper and Row. New York, New York. pp. 3-20.
76. Snodgrass, D. R., W. Smith, E. W. Gray, and J. A. Herring. 1976. A Rotavirus in Lambs with a Diarrhoea. Res. Vet. Sci. 20:113-114.
77. Swift, J. A. and M. N. Marsh. 1968. Scanning Electron Microscopy of Rat Intestinal Microvilli. (Letter). Lancet. 2:915.
78. Thake, D. C. 1969. Jejunal Epithelium in Transmissible Gastroenteritis of Swine: An Electron Microscopic and Histochemical Study. Am. J. Pathol. 53:149-168.
79. Thake, D. C., H. W. Moon, and G. Lambert. 1973. Epithelial Cell Dynamics in Transmissible Gastroenteritis of Neonatal Pigs. Vet. Pathol. 10:330-341.
80. Theil, K. W., E. H. Bohl, A. G. Agnes. 1977. Cell Culture Propagation of Porcine Rotavirus (Reovirus-Like Agent). Am. J. Vet. Res. 38:1765-1768.
81. Theil, K. W., E. H. Bohl, R. F. Cross, E. M. Kohler, and A. G. Agnes. 1978. Pathogenesis of Porcine Rotaviral Infection in Experimentally Inoculated Gnotobiotic Pigs. Am. J. Vet. Res. 39:213-220.
82. Toner, P. G. 1968. Cytology of Intestinal Cells. International Review of Cytology. Ed. Bourne, G. H. and J. F. Daniell. Academic Press. New York, New York. 24:235-343.
83. Toner, P. G. and K. E. Carr. 1969. The Use of Scanning Electron Microscopy in the Study of the Intestinal Villi. J. Pathol. 97:611-617.
84. Torres-Medina, A., R. G. Wyatt, C. A. Mebus, N. R. Underdahl, and A. Z. Zapikian. 1976. Diarrhea Caused in Gnotobiotic Piglets by the Reovirus-Like Agent of Human Infantile Gastroenteritis. J. Infect. Dis. 133:22-27.
85. Trapp, A. L., V. L. Sanger, and E. Stalnaker. 1966. Lesions of the Small Intestinal Mucosa in Transmissible Gastroenteritis-Infected Germfree Pigs. Am. J. Vet. Res. 27:1695-1702.
86. Trautman, A. and J. Fiebiger. 1952. Fundamentals of the Histology of Domestic Animals. Comstock Pub. Associates (Division of Cornell Univ. Press). Ithaca, New York. pp. 199-216.



87. Wagner, J. E., P. D. Beamer, and M. Ristic. 1973. Electron Microscopy of Intestinal Epithelial Cells of Piglets Infected with a Transmissible Gastroenteritis Virus. *Can. J. Comp. Med.* 37:177-188.
88. Waxler, G. L. 1972. Lesions of Transmissible Gastroenteritis in the Pig as Determined by Scanning Electron Microscopy. *Am. J. Vet. Res.* 33:1323-1328.
89. Welch, A. B. and T. L. Thompson. 1973. Physiochemical Characterization of a Neonatal Calf Diarrhea Virus. *Can. J. Comp. Med.* 37:295-301.
90. Woode, G. N. and J. C. Bridger. 1974. Causes of Piglet Enteritis. (Letter). *Vet. Rec.* 95:71.
91. Woode, G. N. and J. C. Bridger. 1975. Viral Enteritis of Calves. *Vet. Rec.* 96:85-88.
92. Woode, G. N., J. C. Bridger, G. A. Hall, J. M. Jones, and G. Jackson. 1976. The Isolation of a Reovirus-Like Agent (Rotaviruses) from Acute Gastroenteritis of Piglets. *J. Med. Microbiol.* 9:203-209.
93. Woode, G. N., J. C. Bridger, J. M. Jones, T. H. Flewett, A. S. Bryden, H. A. Davies, and G. B. B. White. 1976. Morphological and Antigenic Relationships Between Viruses (Rotaviruses) from Acute Gastroenteritis of Children, Calves, Piglets, Mice, and Foals. *Infect. and Immun.* 14:804-810.
94. Wyatt, R. G., V. W. Gill, M. M. Sereno, A. R. Kalica, D. H. VanKirk, R. M. Chanock, and A. Z. Zapikian. 1976. Probable in vitro Cultivation of Human Reovirus-Like Agent of Infantile Diarrhea. *Lancet.* 1:98-99.
95. Zapikian, A. Z., H. W. Kimm, R. G. Wyatt, W. J. Rodriguez, S. Ross, W. L. Cline, R. H. Parrot, and R. M. Chanock. 1974. Reoviruslike Agent in Stools: Association with Infantile Diarrhea and Development of Serologic Tests. *Science.* 185:1049-1053.
96. Zworykin, V. K., J. Hillier, and R. L. Snyder. 1942. A Scanning Electron Microscope. *ASTM Bull.* 117:15-23.